ANALYSIS AND DEVELOPMENT OF INTEGRATED INDEX FOR DIAGNOSIS OF CORONARY ARTERY DISEASE BASED ON HEART RATE SIGNALS

M.Tech. Thesis

By
SURABHI SOOD

DISCIPLINE OF ELECTRICAL ENGINEERING
INDIAN INSTITUTE OF TECHNOLOGY INDORE
JUNE 2016

ANALYSIS AND DEVELOPMENT OF INTEGRATED INDEX FOR DIAGNOSIS OF CORONARY ARTERY DISEASE BASED ON HEART RATE SIGNALS

A THESIS

Submitted in partial fulfillment of the
requirements for the award of the degree
of
Master of Technology
in
Discipline of Electrical Engineering
with specialization in
Communication and Signal Processing
by

SURABHI SOOD

DISCIPLINE OF ELECTRICAL ENGINEERING
INDIAN INSTITUTE OF TECHNOLOGY INDORE
JUNE 2016

INDIAN INSTITUTE OF TECHNOLOGY INDORE

CANDIDATE'S DECLARATION

I hereby certify that the work which is being presented in the thesis entitled "**ANALYSIS AND DEVELOPMENT OF INTEGRATED INDEX FOR DIAGNOSIS OF CORONARY ARTERY DISEASE BASED ON HEART RATE SIGNALS"** in the partial fulfillment of the requirements for the award of the degree of **MASTER OF TECHNOLOGY** and submitted in the **DISCIPLINE OF ELECTRICAL ENGINEERING, Indian Institute of Technology Indore**, is an authentic record of my own work carried out during the time period from JULY, 2015 to JUNE, 2016 under the supervision of Dr. Ram Bilas Pachori, Associate Professor, Discipline of Electrical Engineering, IIT Indore.

The matter presented in this thesis has not been submitted by me for the award of any other degree of this or any other institute.

Signature of the student with date
SURABHI SOOD

This is to certify that the above statement made by the candidate is correct to the best of my knowledge.

Signature of the Supervisor with date

DR. RAM BILAS PACHORI

SURABHI SOOD has successfully given her M.Tech. Oral Examination held on **29-06-2016**.

Signature of Supervisor of M.Tech. Thesis
Date:

Convener, DPGC
Date:

Signature of PSPC Member
Date:

Signature of PSPC Member
Date:

ACKNOWLEDGEMENTS

First of all, I would like to express my sincere gratitude to my thesis supervisor **Dr. Ram Bilas Pachori** for his constant support and guidance throughout this work and **Prof. U. Rajendra Acharya, Department of Electronics and Computer Engineering, Ngee Ann polytechnic, Singapore** for providing the database which has been studied in this work.

I would also like to express my gratitude to my PSPC committee members **Dr. Vivek Kanhangad** and **Dr. Anand Parey** for their valuable suggestions.

I would also like to thank entire Discipline of Electrical Engineering for providing all the facilities and resources.

I would also like to thank all the faculty members of Electrical Engineering Department for teaching me during my course work which led to strong foundation for this work.

I would also like to thank **Mr. Mohit Kumar,** Ph. D student for their assistance at various stages of this work.

I am also thankful to all the members of Signal Analysis Lab for all their assistance.

I would also like to thank all the students of Electrical Engineering Research Lab for their help and guidance.

I would like to express my appreciation to my batch mates **Satyartha**, **Kapil** and **Anchal** for me providing the emotional support and encouraging me through motivating and thoughtful discussions.

I am especially grateful to my family for their support and for believing in me.

SURABHI SOOD
(1402102012)

M.Tech. (Communication and Signal Processing)

Discipline of Electrical Engineering

IIT Indore

Dedicated

to

My Family and Friends

Abstract

Coronary Artery Disease (CAD) is one of the very common type of cardiovascular diseases which is the killer of world's 7.4 million population. Coronary artery disease is characterized by the narrowing and hardening of arteries supplying blood to the muscles of heart, owing to the deposition of waxy substance called plaque in them. The consequence of coronary artery disease may be a heart attack or heart stroke. Hence, the patient's suffering from coronary artery disease are always at the risk of death. In the world, where trained cardiologists may diagnose coronary artery disease with manual errors, computer aided diagnostics methods may be of great help. Thus in this thesis we have proposed an efficient way to diagnose coronary artery disease using heart rate signals. We have used Empirical Mode Decomposition (EMD) to decompose the heart rate signal into Intrinsic Mode Functions (IMFs). The features namely: Area of Second Order Difference Plot (SODP area), Area of Analytical Signal Representation (ASR area), Amplitude Modulation (AM) bandwidth, Frequency Modulation (FM) bandwidth and Fourier Bessel expansion (FBE) based mean frequency are extracted from these IMFs of different signals. These features are then subjected to Kruskal-Wallis statistical test to check their statistical significance.

In the next part of this work, we have used the same dataset and derived the modes of each signal using Empirical Wavelet Transform (EWT). The same set of features is derived from these obtained modes of the signals. These features are again tested for their statistical significance and the best three features are selected to derive an integrated index for discrimination between normal and coronary artery disease heart rate signals using a single value.

LIST OF PUBLICATIONS

1. S. Sood, M. Kumar, R. B. Pachori and U. R. Acharya, Application of empirical mode decomposition based features for analysis of normal and CAD heart rate signals, *Journal of Mechanics in Medicine and Biology* vol. 16, no. 01 (2016) 1640002.

CONTENTS

LIST OF FIGURES

LIST OF TABLES

CHAPTER 1

Introduction

Every human organ requires oxygen and nutrients to be in a healthy condition and function properly, including heart. This oxygen is provided to every cell and tissue of the body through blood which contains dissolved oxygen and nutrients in it. In one cardiac cycle of the heart the deoxygenated blood from whole body is brought to the heart, this blood is given from right ventricle to the lungs for oxygenation (adding oxygen to the blood from the air we breathe) and brought back to the heart in left atrial and further distributed to whole body through left ventricle [1]. This cycle continues without any disruption. Heart regulates the blood flow through the network of blood vessels. Blood vessels are of two types: (a). Arteries, which carries oxygenated blood from heart to the body and (b). Veins, which carries deoxygenated blood from the body to heart [2]. Any blockage in arteries or veins would disrupt the proper functioning of heart which may lead to various cardiovascular diseases [1, 2].

Cardiovascular diseases are responsible for 17 million deaths across the world every year, out of which most of the deaths are the results of Coronary Artery Disease (CAD) [1], most common kind of cardiovascular diseases. Early diagnosis of CAD can save many lives.

1.1 Cardiovascular Disease and Its Types:

Cardiovascular diseases are disorders involving heart and blood vessels such as: Cerebrovascular Disease, which is related to the blood vessels supplying to the brain [3]. Peripheral artery disease, which is related to infection of blood vessels supplying to the arms and legs and if the blood vessels supplying to the heart muscles itself is infected then the condition is said to be CAD [3]. Cardiovascular disease leads to more deaths in the world than any other disease. In 2012, due to cardiovascular diseases the death toll was estimated to be 17.5 million out of which CAD contributed to 7.4 million deaths [3].

1.2 Coronary Artery Disease: Causes, Symptoms and Diagnosis

The CAD is a heart condition in which a waxy substance called plaque is deposited in the artery carrying blood to the heart muscles [2]. The plaque is deposited due to unhealthy eating habits, tobacco use, physical inactivity and drinking habit [1]. With time this plaque deposited inside arteries hardens them. This results in narrowing of the arteries which hinders the supply of blood and oxygen to the heart muscles [1]. When heart muscles do not get the proper amount of oxygen, it exhausts the cells and tissues of heart which may result in strokes and heart attacks. This may slowly and eventually lead to the death of an individual. The symptoms of CAD may involve chest pain, shortness of breath and fatigue.

CAD can be diagnosed on the basis of some clinical tests and physical examination. These include Exercise Stress Test (EST), coronary angiography, Electrocardiogram (ECG), cardiac catheterization, blood tests and chest X-rays [2, 4]. In EST, a patient is given some physical exercise such as walking on a tread mill and hence, targeted heart rate is to be achieved by the heart. This may increase the work load of heart [5]. This method is not preferred as it may give a normal ECG recording even for a person suffering from CAD [4]. The other techniques such as angiography and cardiac catheterization are invasive, causing pain and discomfort to the body [2, 4]. Moreover, these methods can be performed by trained persons only. Hence, developing any method which may avoid invasion of body is recommended and in that case analysis of Heart Rate Variability (HRV) using signal processing method is very useful.

Time variation of heart rate between successive heartbeats in ECG signal is called HRV signal [6]. HRV signal is complex in nature. Linear statistical measures like standard deviation, mean and variance may miss some small but useful information [4]. It was shown that circadian rhythm in HRV is reduced in CAD patients than normal patients [7].

1.3 Electrocardiogram

The ECG is the simple and painless test which records the electrical activity of the heart [4]. This electrical signal originate from sinus node and travel through the length of heart. Once the

signal has travelled the entire length, it constitute a heartbeat [4]. The complete process is repeated and form a periodic signal called electrocardiogram signal, consisting of repeated pulses.

A normal ECG recording consist of P-wave followed by QRS-complex and T-wave. P-wave occur due to left and right atrial depolarization whereas left and right ventricular depolarization causes QRS-complex [4]. T-wave corresponds to ventricular repolarization. R-wave has the maximum amplitude [4].

1.4 Related Work

Giri et al. [5] used data reduction techniques on the discrete wavelet transform coefficients. Better classification result is obtained with independent component analysis and Gaussian mixture model classifier. Acharya et al. [6] studied the results of the nonlinear analysis on CAD HRV signals to show more rhythmic nature of CAD HRV signals than normal signals. Acharya et al. [7] presented various nonlinear and linear parameters for the analysis of cardiac abnormalities of eight different types with more than 90% confidence level. Huikiri et al. [8] studied the effects of upright and arousal postures in circadian rhythm of CAD affected patients. They also used the heart rate variability signals. Bigger et al. [9] studied HRV signals of CAD and normal subjects and analyzed them in time and frequency domain. All parameters in these domain are found lower in CAD patients. Various nonlinear methods are applied to analyze the HRV signals due to its nonlinear nature [10, 11, 12, 13, 14].

Acharya et al. [10] studied various cardiac abnormalities and analyzed them using scalogram plots and FD. Scalogram plots and values of FD are unique for each abnormalities. Karamanos et al. [11] used block entropy to examine the coarse-grained statistics of CAD and normal HRV signals. For normal subject, more complex statistics are observed than CAD subjects. Chua et al. [15] studied Higher Order Spectrum (HOS) on HRV signals of seven different cardiac arrhythmia, and unique bi-spectrum plots are proposed for these classes of arrhythmia. Antanavicius et al. [12] found Fractal Dimension (FD), embedding dimension error, recurrence dimension and mutual information to be lower for non-CAD subjects. Babaoglu et al. [16] studied Binary Particle Swarm Optimization (BPSO) and Genetic Algorithm (GA)-based feature extraction method combined with SVM classifier for diagnosing CAD.

Patidar et al. [13] studied the values of correntropy and found them to be lower for CAD HRV signals than normal HRV signals. Lee et al. [17] used various classifiers to test the linear and nonlinear features extracted from HRV signals of normal and CAD subjects, and found better results with support vector machine classifier.

1.5 Thesis Organization

The rest of thesis is organized as below:

Chapter 2 gives detailed description of EMD based feature analysis, its methodology, results and discussion. Chapter 3 includes EWT based derivation of integrated index, its results and discussion. In the end chapter 4 gives conclusion and the future scope of the present work followed by the references.

CHAPTER 2

Empirical Mode Decomposition based Analysis of Normal and CAD Signals

Computer aided diagnosis is performed on the normal and CAD signals as firstly, the EMD is applied to the two classes of signals and then five features namely, Area of Second Order Difference Plot (SODP area), Area of Analytical Signal Representation (ASR area), Amplitude Modulation (AM) bandwidth, Frequency Modulation (FM) bandwidth and Fourier Bessel Expansion (FBE) based mean frequency are extracted from the Intrinsic Mode Functions (IMFs). These features are studied individually and Kruskal-Wallis statistical test [18] is applied to them. Features giving *p*-values less than 0.05 are considered to be significant.

2.1 Data Acquisition

Normal and CAD ECG signals were acquired using BIOPAC [19] instrument at Iqraa hospital, Kerela, India. These signals are sampled at a rate of 500 Hz. The average age for both classes is 50 years varying from 40 to 70 years. The ECG signals from 10 CAD and 10 normal subjects were recorded out of which 61 normal and 82 CAD signals files were formed with each file containing 1000 samples. The subjects suffering from hypertrophy, atrial fibrillation, congestive heart failure, bundle branch block and myopathy were excluded from CAD subjects.

ECG signal thus obtained contains power line interference, baseline wanders [20] and unwanted noise. These can be removed using band pass filters having higher cut off frequency of 15 Hz and lower cut off frequency of 0.3 Hz. Band stop filter with cut off frequency of 50 Hz is also used. The time interval (T_{RR}) between consecutive R peaks is calculated as RR interval and R peaks is found using Pan-Tompkins Algorithms [21]. Finally Heart Rate (in beats per minute) = $60/T_{RR}$ is calculated. Figure 2.1 depicts CAD and a normal heart rate signal.

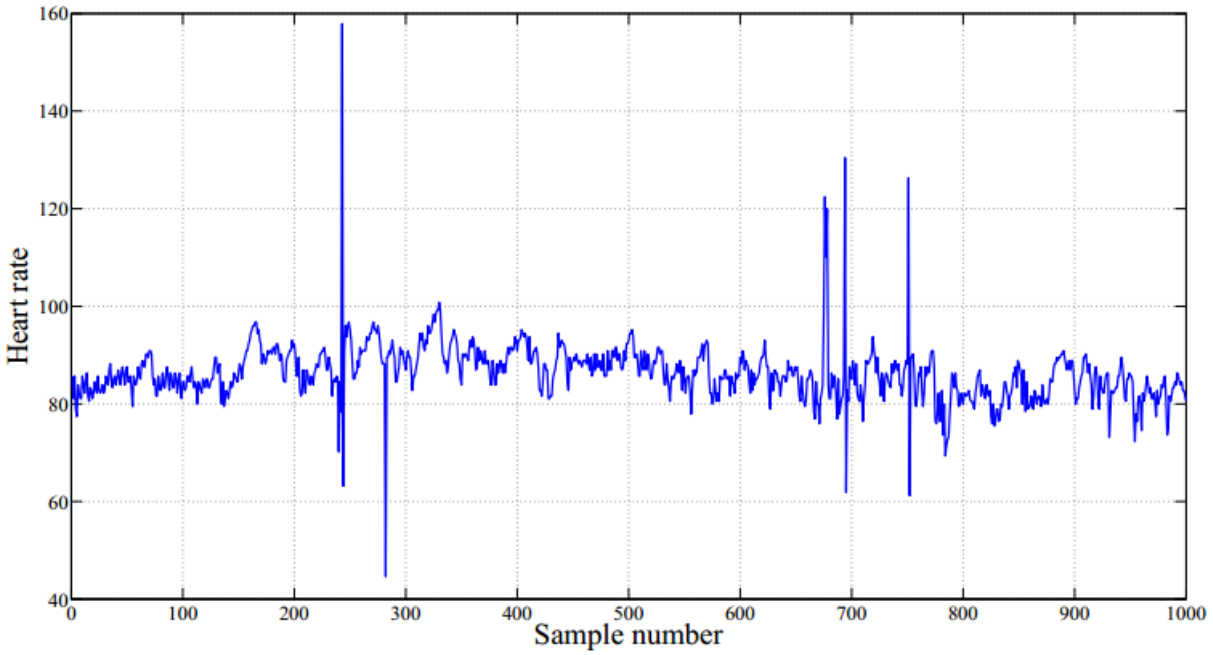

(a)

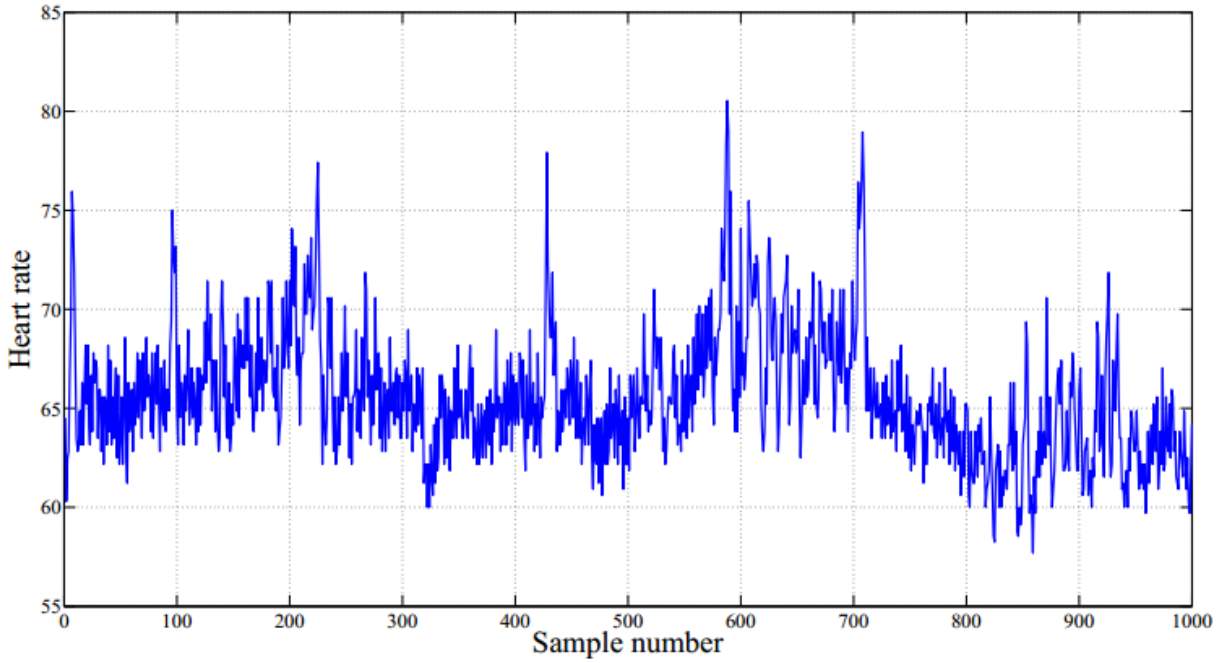

(b)

Figure 2.1: The heart rate signal of (a) CAD and (b) Normal subject.

2.2 Empirical Mode Decomposition

Every non-stationary signal is assumed to be made up of different oscillatory components which can be derived using EMD technique [22]. Hence, EMD is a technique to decompose a non-stationary and nonlinear signal into its constituting signals which are termed as IMFs [22]. The IMFs are frequency and amplitude modulated signals. These IMFs can be derived from a signal $z(t)$ using sifting process as explained in [22]:

The EMD method can be represented by the following steps [22, 23]:

Step 1. Locate local minima and local maxima in signal $z(t)$

Step 2. Form $U(t)$, upper envelope by joining the local maxima and similarly $L(t)$, lower envelope by joining the local minima.

Step 3. Calculate the signal formed by averaging the upper envelope and lower envelope as: $\mu(t) = \frac{U(t)+L(t)}{2}$

Step 4. Subtract the mean signal $\mu(t)$ from the original signal $z(t)$: $I(t) = z(t) - \mu(t)$

Step 5. Check whether $I(t)$ is the desired IMF by testing it for two necessary IMF conditions. They are:

1. The number of maxima and minima must be equal to the number of zero crossings in the signal $I(t)$ or differ at most by one.
2. The average value of upper envelope of local maxima and lower envelope of local minima at any point in $I(t)$ must be zero.

Step 6. If $I(t)$ does not satisfy the above conditions then repeat the steps (a) to (e) till the signal $I(t)$ is obtained which satisfies the IMF conditions. This signal is considered the first IMF denoted by IMF_1.

Step 7. The remaining IMFs are obtained from the residual signal given as:

$r(t) = z(t) - \text{IMF}_1$ using the same sifting process.

Step 8. The complete process is continued till the residual signal becomes monotonic and no further IMFs can be derived from it.

Step 9. Finally, the signal $z(t)$ can be expressed as:

$$z(t) = \sum_{i=1}^{N} \text{IMF}_i + R(t) \quad (2.1)$$

where, i gives the number of IMFs obtained from sifting process and $R(t)$ gives the final residue signal which further cannot be decomposed into IMFs.

The IMFs of normal and CAD signal are shown in the Figure 2.2.

2.3 Features Extracted

The features extracted from the obtained IMFs are given in detail below.

2.3.1 Area of Second Order Difference Plot

The Second Order Difference Plot (SODP) is defined as the graphical representation of first order derivative and the second order derivate of the signal against each other [24, 25]. The graphical shape of SODP of the IMFs is elliptical. The area of these SODPs corresponding to 95% Central Tendency Measures (CTM) [26, 27] is used in this work to analyze the normal and CAD classes. The SODP of any signal $z(j)$ is computed as [24]:

$$P(j) = z(j+1) - z(j) \quad (2.2)$$

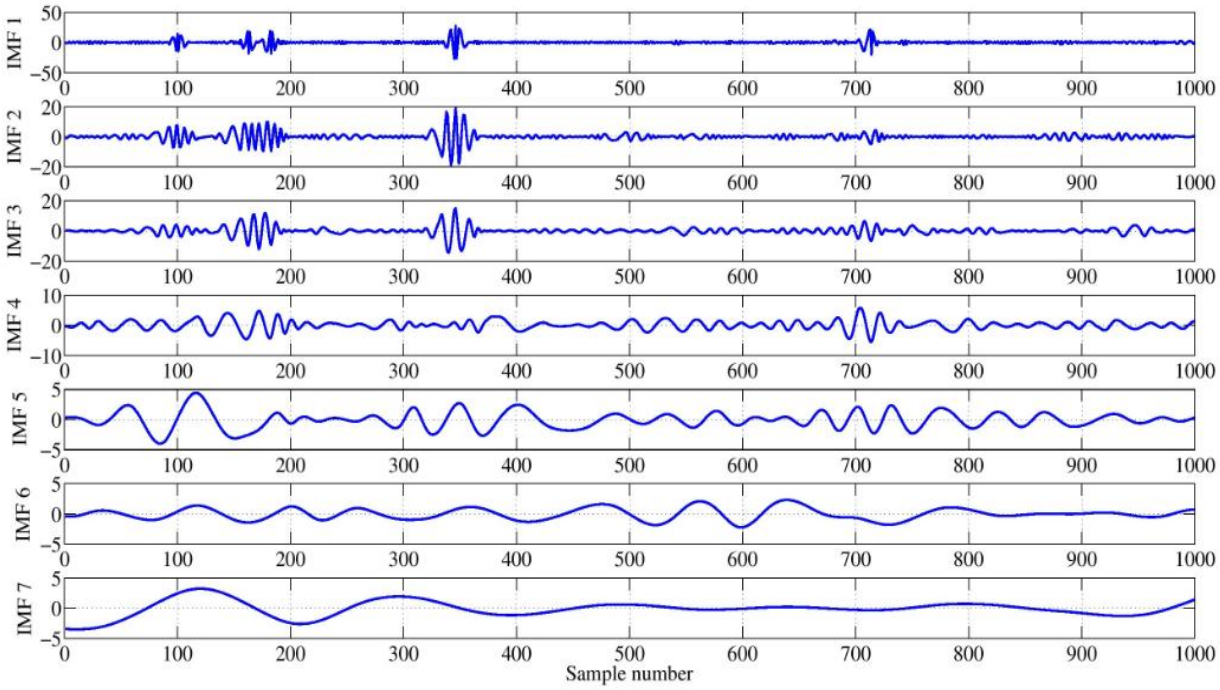

(a)

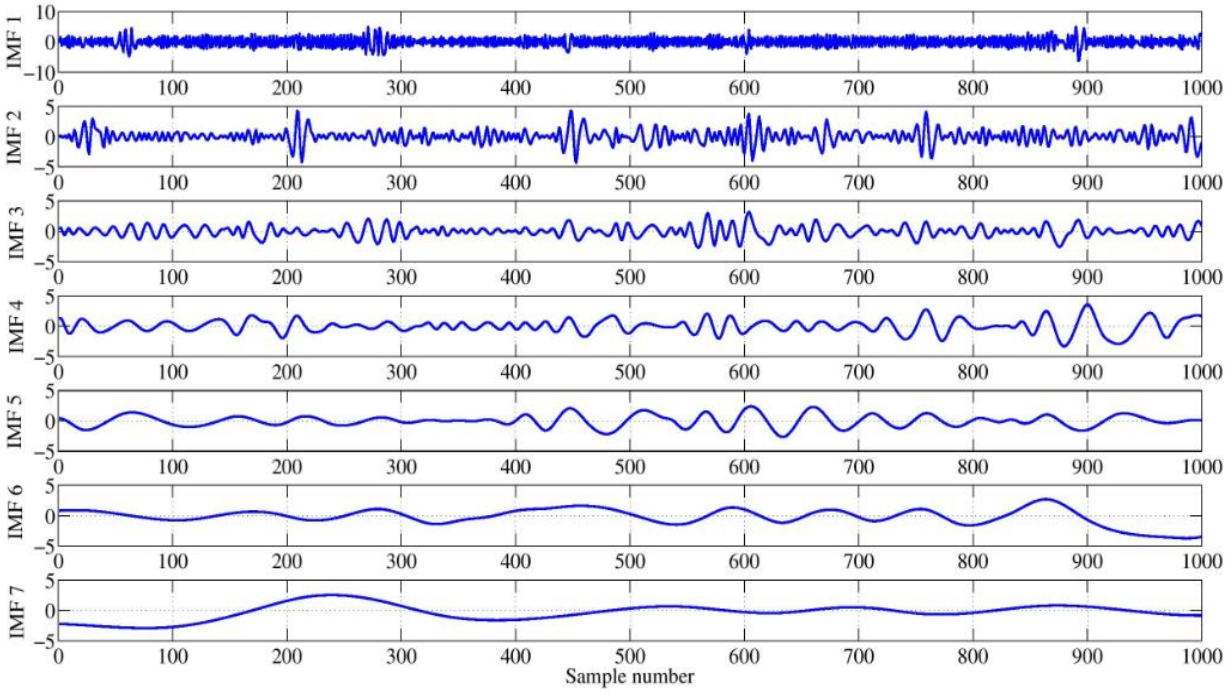

(b)

Figure 2.2: First 7 IMFs obtained with EMD of (a) CAD subject and (b) Normal subject.

$$Q(j) = z(j+2) - z(j+1) \tag{2.3}$$

Where, $P(j)$ and $Q(j)$ are first order and second order derivatives of signal $z(j)$. Plotting $P(j)$ and $Q(j)$ against each other will give SODP.

The steps to compute 95% ellipse area [28, 29, 30, 31] of SODP thus obtained are given below:

1. Calculate mean of $P(j)$ and $Q(j)$ as:

$$M_P = \sqrt{\frac{1}{N}\sum_{j=0}^{N-1} P(j)^2} \tag{2.4}$$

$$M_Q = \sqrt{\frac{1}{N}\sum_{j=0}^{N-1} Q(j)^2} \tag{2.5}$$

$$M_{PQ} = \frac{1}{N}\sum P(j)\, Q(j) \tag{2.6}$$

2. Calculate parameter X as:

$$X = \sqrt{\left({M_P}^2 + {M_Q}^2\right) - 4({M_P}^2{M_Q}^2 - {M_{PQ}}^2)} \tag{2.7}$$

3. Parameter D and E are calculated as:

$$D = 1.732\sqrt{\left({M_P}^2 + {M_Q}^2\right) + X} \tag{2.8}$$

$$E = 1.732\sqrt{\left({M_P}^2 + {M_Q}^2\right) - X} \tag{2.9}$$

4. Area of the ellipse is:

$$\text{SODP area} = \pi DE \tag{2.10}$$

2.3.2 Area of Analytical Signal Representation

The ASR of any signal $z(t)$ is a complex signal with its real part as the signal itself and the imaginary part as its Hilbert transform [32]. The ASR of a signal is circular in nature with a unique center [33]. In this work we have calculated the area of ASR corresponding to 95% CTM [33]. CTM correspond to the number of points lying within the chosen radius to the total points in ASR of IMFs of the signal. The computational steps for calculating the area of ASR are given below [33, 34, 35, 36]:

Step 1. The analytical signal representation of a signal $z(t)$ is given by:

$$O(t) = z(t) + jz_h(t) \tag{2.11}$$

This can also be written as:

$$O(t) = Z(t)e^{i\theta(t)} \tag{2.12}$$

Here, $Z(t)$ is the magnitude of analytical signal representation $O(t)$ and $\theta(t)$ is the angle of signal $z(t)$. The expression for $Z(t)$ and $\theta(t)$ are as follows:

$$Z(t) = \sqrt{z^2(t) + {z_h}^2(t)} \tag{2.13}$$

$$\theta(t) = \tan^{-1}\left[\frac{z_h(t)}{z(t)}\right] \tag{2.14}$$

Step 2. CTM is given by:

$$\text{CTM} = \frac{\sum_{m=1}^{M} n(m)}{M} \tag{2.15}$$

Where, $$n(m) = \begin{cases} 1, & \left(\left[\text{re}\left(O(t)\right)\right]^2 + [\text{im}(O(t))]^2\right)^{1/2} < a \\ 0, & \text{otherwise} \end{cases}$$

Here, a is the chosen radius and $n(m)$ denotes the number of points lying within the chosen radius. Now, the radius (say R) which gives the 95% CTM is considered to find the area of ASR.

Step 3. Area of ASR denoted by ASR area is given by:

$$\text{ASR area} = \pi R^2 \tag{2.16}$$

2.3.3 Amplitude and Frequency Modulation Bandwidths

As stated earlier the IMFs of any signal obtained from EMD technique are amplitude and frequency modulated oscillatory signals [22]. This clearly implies that the IMFs have amplitude and frequency modulation bandwidths. The amplitude modulated bandwidth refers to the spread in signal frequencies due to amplitude variations and frequency modulation bandwidth refers to the spread of frequencies due to deviation from central frequency of the signal [37]. We know that $B^2 = {B_{AM}}^2 + {B_{FM}}^2$ where, B is bandwidth of the signal, B_{AM} is amplitude modulated bandwidth and B_{FM} is frequency modulated bandwidth [37, 38]. Bandwidth of a signal is also given by:

$$B^2 = \frac{1}{E}\int \left(\frac{dZ(t)}{dt}\right)^2 dt + \frac{1}{E}\int \left(\left(\frac{d\theta(t)}{dt} - < \omega >\right) Z(t)\right)^2 dt \tag{2.17}$$

Hence,
$${B_{AM}}^2 = \frac{1}{E}\int \left(\frac{dZ(t)}{dt}\right)^2 dt \tag{2.18}$$

$${B_{FM}}^2 = \frac{1}{E}\int \left(\left(\frac{d\theta(t)}{dt} - < \omega >\right) Z(t)\right)^2 dt \tag{2.19}$$

Here, E signifies energy of the signal. For calculating amplitude and frequency modulation bandwidths, we need to calculate $Z(t)$ and $\theta(t)$ which is shown in the previous sections. Hence, B_{AM} and B_{FM} of IMFs are used to analyze normal and CAD subjects effectively.

2.3.4 Mean Frequency Computed using Fourier-Bessel Expansion

The mean frequency of the signal in this work is calculated using Fourier-Bessel expansion. The Fourier-Bessel coefficients are unique for a signal [39]. The computation of mean frequency (MF) involves steps which are listed below [40]:

$$MF = \frac{\sum_{j=1}^{K} F_j E_j}{\sum_{j=1}^{K} E_j} \tag{2.20}$$

The parameters F_j and E_j are frequency and energy of the j[th] coefficient. They can be expressed mathematically as [39, 40]:

$$F_j = \frac{\gamma_j}{2\pi T} \tag{2.21}$$

And,

$$E_j = \frac{{C_j}^2 [J_1(\gamma_j)]^2 T^2}{2} \tag{2.22}$$

γ_j are the roots of $J_0(\gamma) = 0$. Mean frequency represents the center frequency or centroid of the desired signal's frequency spectrum [41-47]. The mean frequency measure of IMFs is used to analyze normal and CAD signals in this work.

In this work, after extracting these above mentioned features from the IMFs of the normal and CAD signals, we have applied Kruskal-Wallis statistical test to them and *p*-values are noted. The features having *p*-value less than 0.05 are considered to be significant and can distinguish well between normal and CAD signals.

2.4 Results

In the present work, CAD and normal signals are analyzed for three different signal lengths 1000, 500 and 250 samples. Firstly, we obtained IMFs by applying EMD method on these signals. Further, five features namely; SODP area, ASR area, AM bandwidth, FM bandwidth and FBE-based mean frequency are computed from these IMFs. The effectiveness of these features for analyzing normal and CAD signals are tested by observing the *p*-values computed using Kruskal-

Wallis statistical test. The features with *p*-values less than 0.05 are considered statistically significant.

Table 2.1: *p*-values of features extracted from different IMFs for normal and CAD signals with 1000 samples.

Features	IMF 1	IMF 2	IMF 3	IMF 4	IMF 5	IMF 6	IMF 7
SODP area	7.7×10^{-1}	5.0×10^{-1}	5.5×10^{-1}	4.4×10^{-1}	8.8×10^{-1}	8.4×10^{-1}	5.6×10^{-1}
ASR area	8.5×10^{-1}	6.4×10^{-1}	6.2×10^{-1}	8.7×10^{-1}	3.4×10^{-1}	7.2×10^{-2}	1.9×10^{-1}
AM bandwidth	4.3×10^{-7}	4.6×10^{-1}	1.0×10^{-3}	1.4×10^{-1}	7.8×10^{-1}	3.7×10^{-1}	1.9×10^{-1}
FM bandwidth	8.2×10^{-4}	2.5×10^{-3}	8.6×10^{-2}	4.2×10^{-4}	4.3×10^{-3}	6.7×10^{-3}	3.3×10^{-4}
FBE-based mean frequency	3.5×10^{-1}	1.4×10^{-4}	4.8×10^{-2}	7.7×10^{-5}	5.5×10^{-5}	1.7×10^{-6}	3.3×10^{-4}

For signal with 1000 samples, at least seven IMFs are present for normal and CAD signals. In case of signal with 500 samples, all normal and CAD signals have at least six IMFs. For signals with 250 samples also, at least six IMFs are present for normal and CAD signals. The box plots for the sample length of 1000, 500 and 250 samples are also shown in Figure 2.3 - 2.17. The corresponding *p*-values are shown in Table 2.1, 2.2 and 2.3 respectively.

Table 2.2: *p*-values of features extracted from different IMFs for normal and CAD signals with 500 samples.

Features	IMF 1	IMF 2	IMF 3	IMF 4	IMF 5	IMF 6
SODP area	1.3×10^{-1}	3.8×10^{-2}	2.5×10^{-1}	2.0×10^{-1}	4.1×10^{-1}	2.1×10^{-1}
ASR area	7.1×10^{-3}	2.4×10^{-2}	9.8×10^{-1}	6.2×10^{-1}	3.5×10^{-1}	2.7×10^{-2}
AM bandwidth	3.2×10^{-8}	4.4×10^{-1}	4.9×10^{-2}	8.2×10^{-1}	5.2×10^{-1}	2.6×10^{-2}
FM bandwidth	3.3×10^{-3}	6.7×10^{-3}	4.8×10^{-1}	3.8×10^{-2}	8.4×10^{-1}	6.2×10^{-1}
FBE-based mean frequency	3.0×10^{-1}	5.6×10^{-8}	1.1×10^{-1}	1.7×10^{-2}	1.8×10^{-2}	1.1×10^{-3}

Table 2.3: *p*-values of features extracted from different IMFs for normal and CAD signals with 250 samples.

Features	IMF 1	IMF 2	IMF 3	IMF 4	IMF 5	IMF 6
SODP area	5.9×10^{-2}	6.3×10^{-3}	6.1×10^{-2}	1.6×10^{-2}	1.1×10^{-1}	4.1×10^{-2}
ASR area	4.8×10^{-2}	2.0×10^{-2}	3.5×10^{-1}	2.9×10^{-1}	6.5×10^{-2}	2.1×10^{-2}
AM bandwidth	6.8×10^{-5}	5.0×10^{-1}	1.5×10^{-1}	5.6×10^{-1}	5.4×10^{-1}	8.5×10^{-2}
FM bandwidth	5.2×10^{-2}	1.8×10^{-2}	4.7×10^{-1}	8.0×10^{-2}	7.5×10^{-1}	3.2×10^{-2}
FBE-based mean frequency	6.6×10^{-1}	1.1×10^{-4}	8.9×10^{-1}	3.6×10^{-2}	1.3×10^{-1}	5.0×10^{-2}

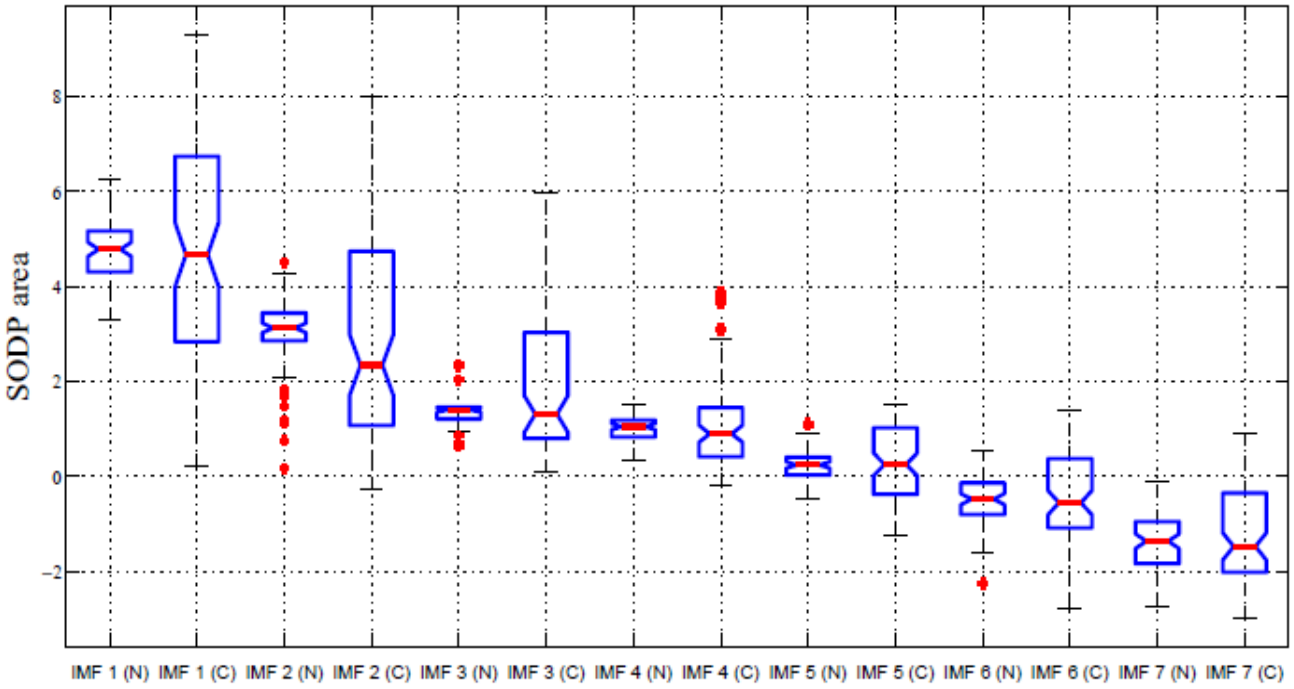

Figure 2.3: Box-plot of SODP area for normal and CAD heart rate signals with 1000 samples.

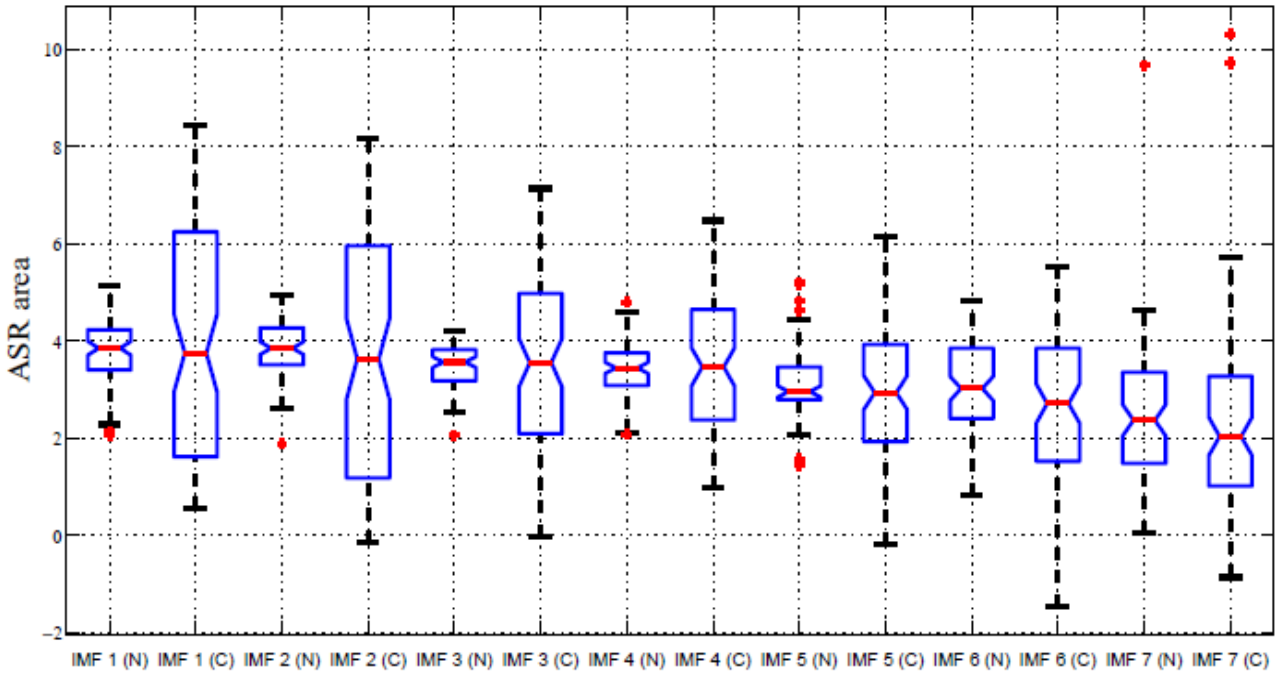

Figure 2.4: Box-plot of ASR area for normal and CAD heart rate signals with 1000 samples.

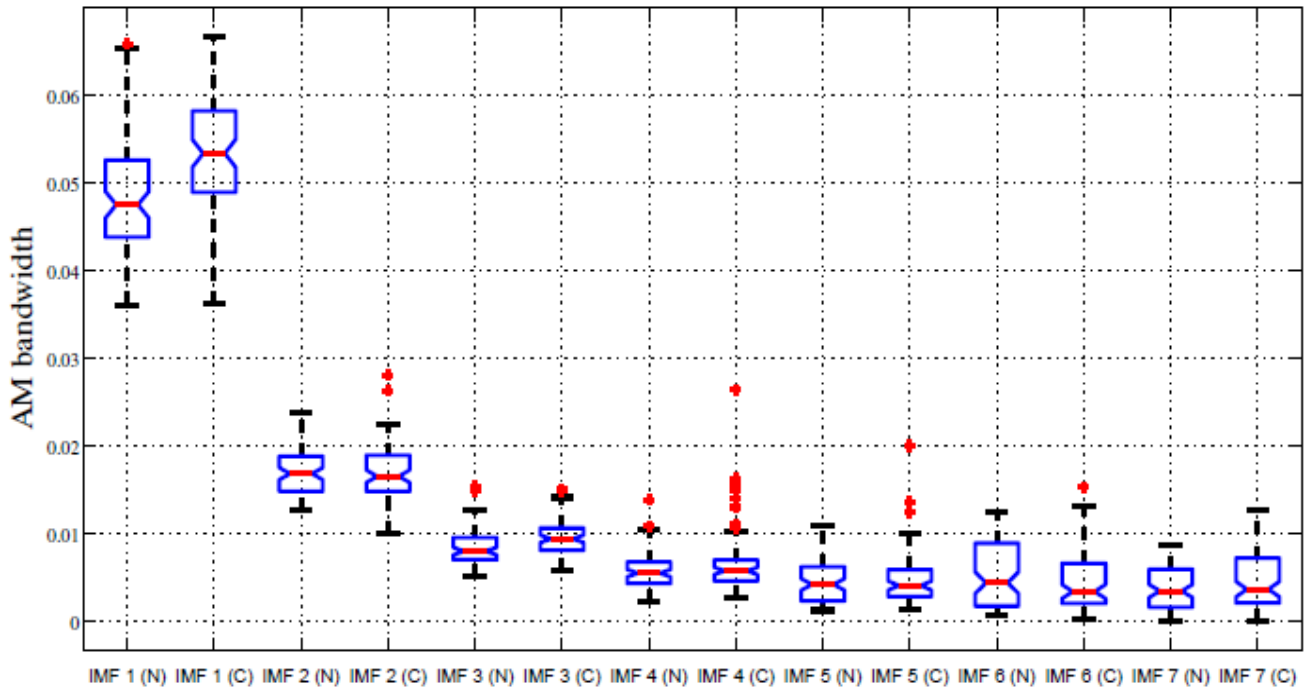

Figure 2.5: Box-plot of AM bandwidth for normal and CAD heart rate signals with 1000 samples.

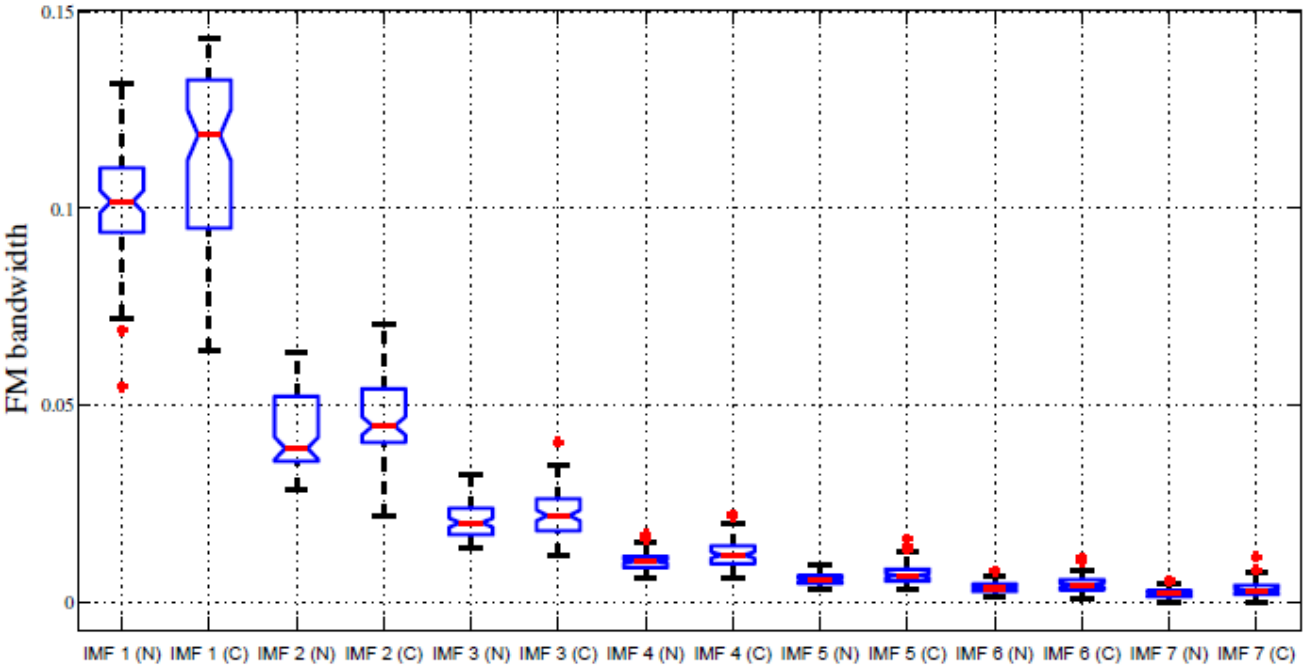

Figure 2.6: Box-plot of FM bandwidth for normal and CAD heart rate signals with 1000 samples.

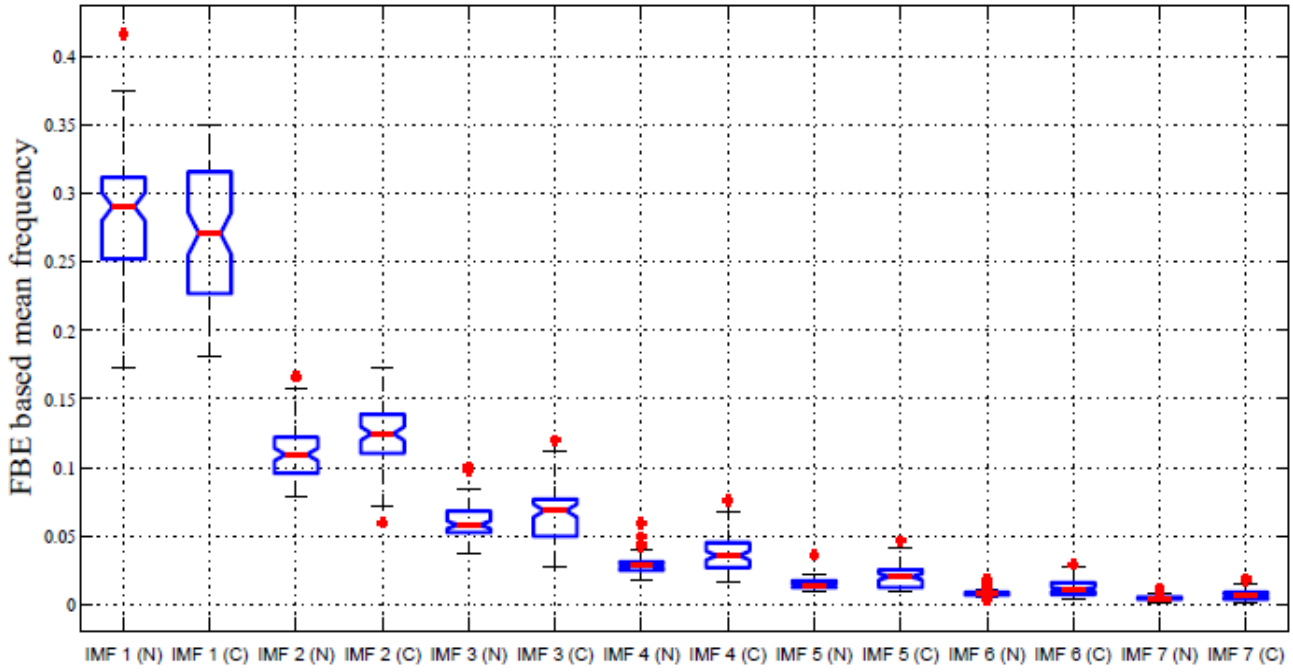

Figure 2.7: Box-plot of FBE based mean frequency for normal and CAD heart rate signals with 1000 samples.

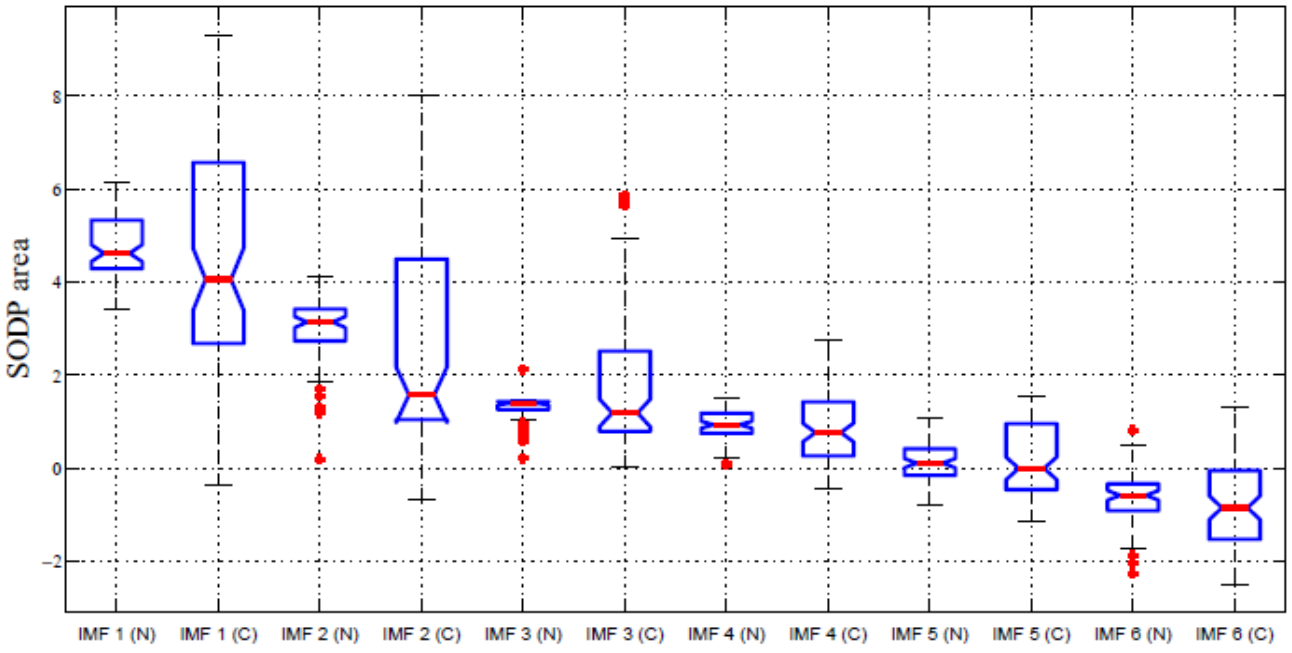

Figure 2.8: Box-plot of SODP area for normal and CAD heart rate signals with 500 samples.

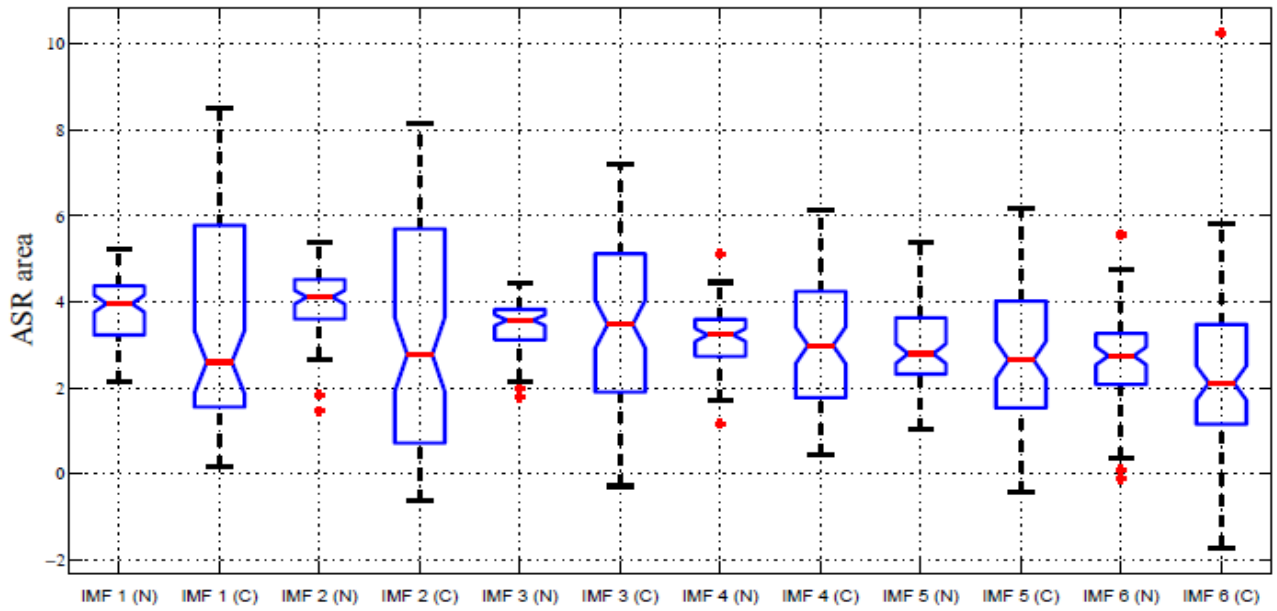

Figure 2.9: Box-plot of ASR area for normal and CAD heart rate signals with 500 samples.

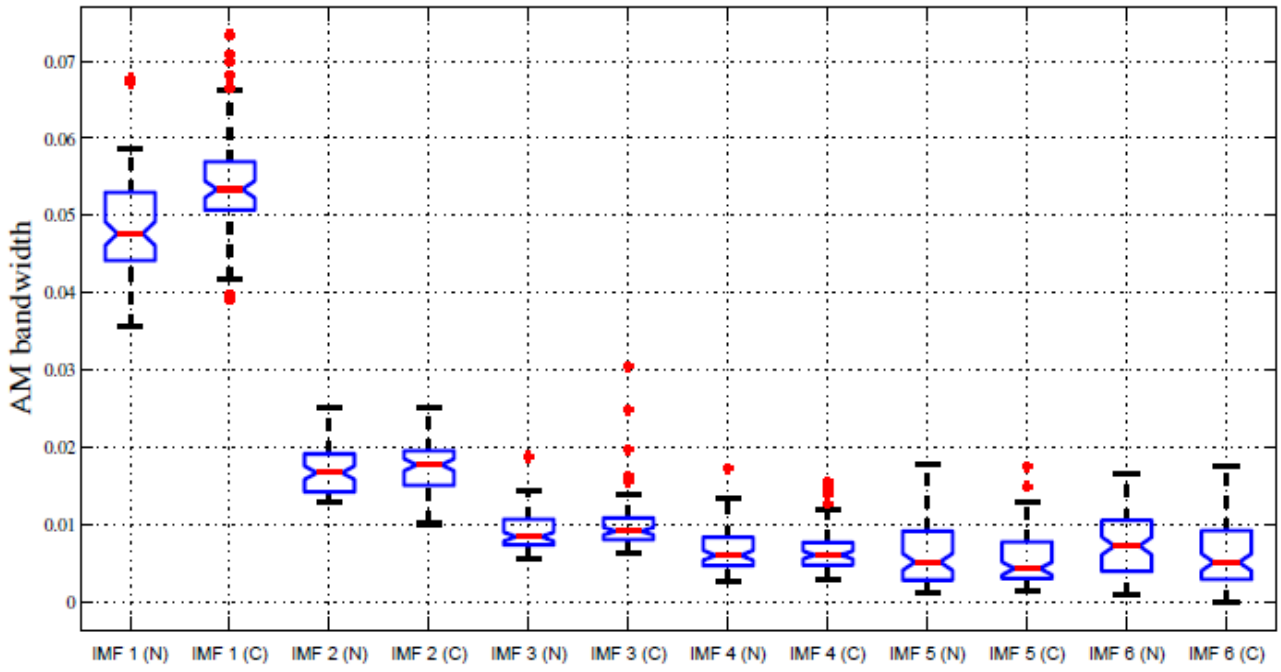

Figure 2.10: Box-plot of AM bandwidth for normal and CAD heart rate signals with 500 samples.

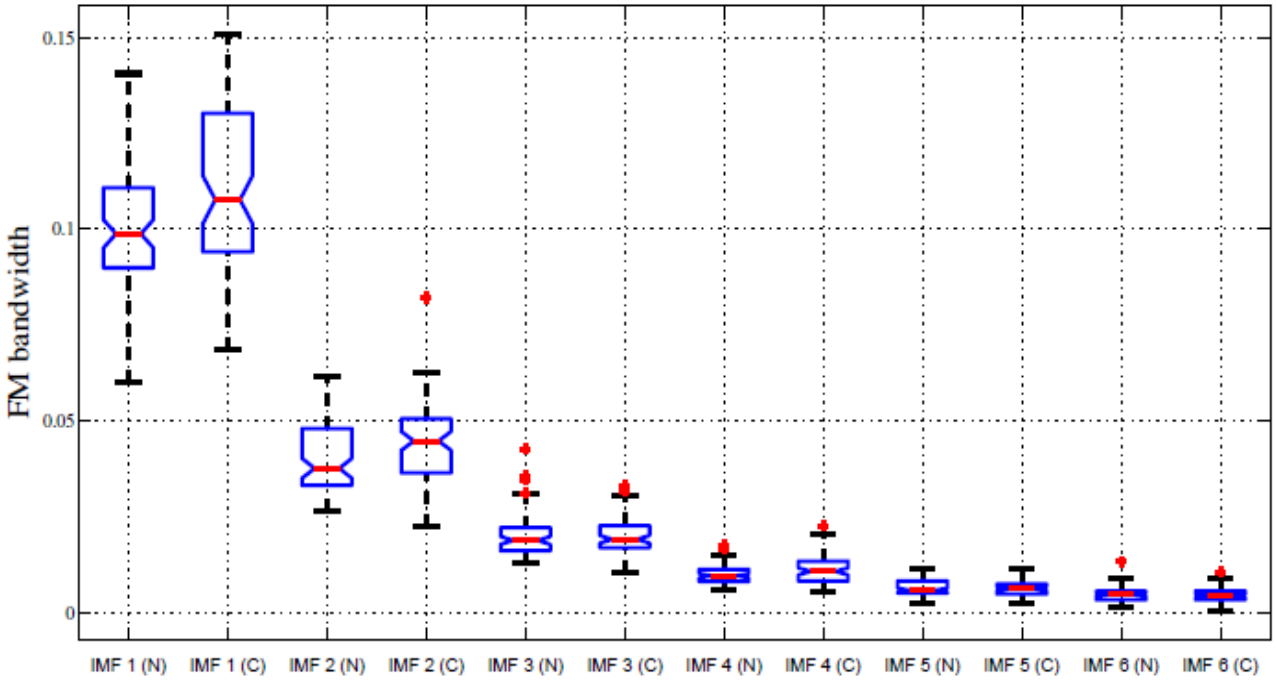

Figure 2.11: Box-plot of FM bandwidth for normal and CAD heart rate signals with 500 samples.

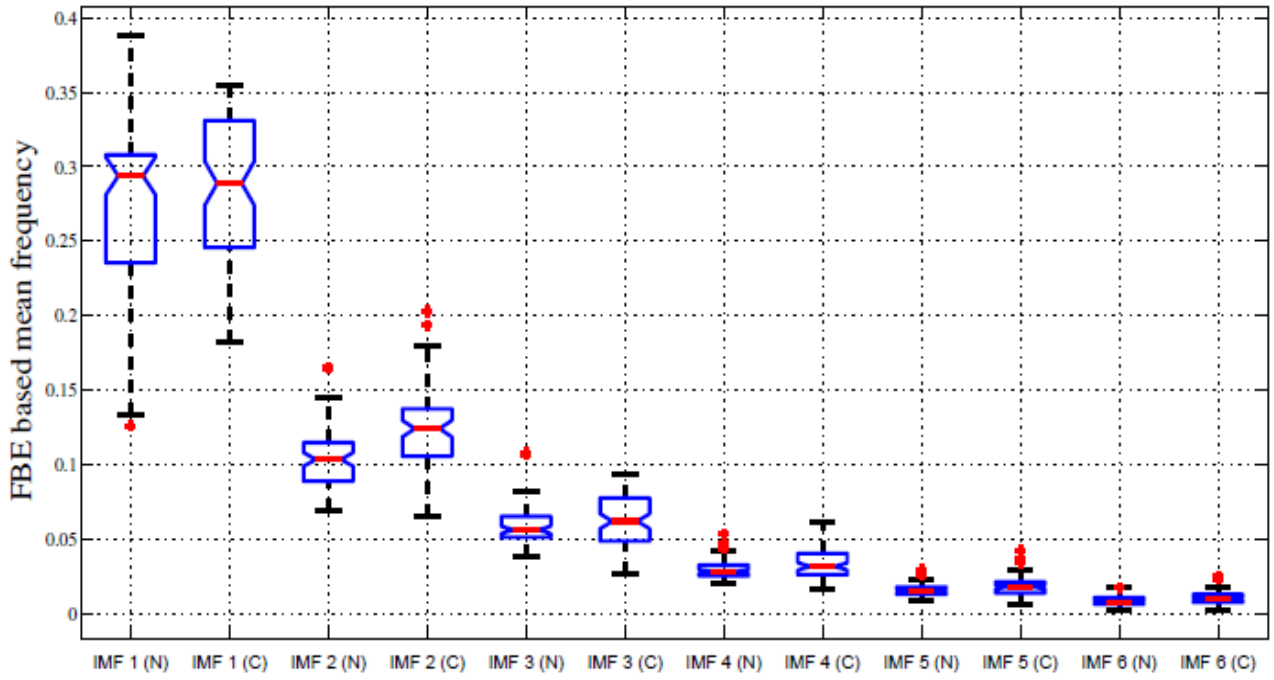

Figure 2.12: Box-plot of FBE based mean frequency for normal and CAD heart rate signals with 500 samples.

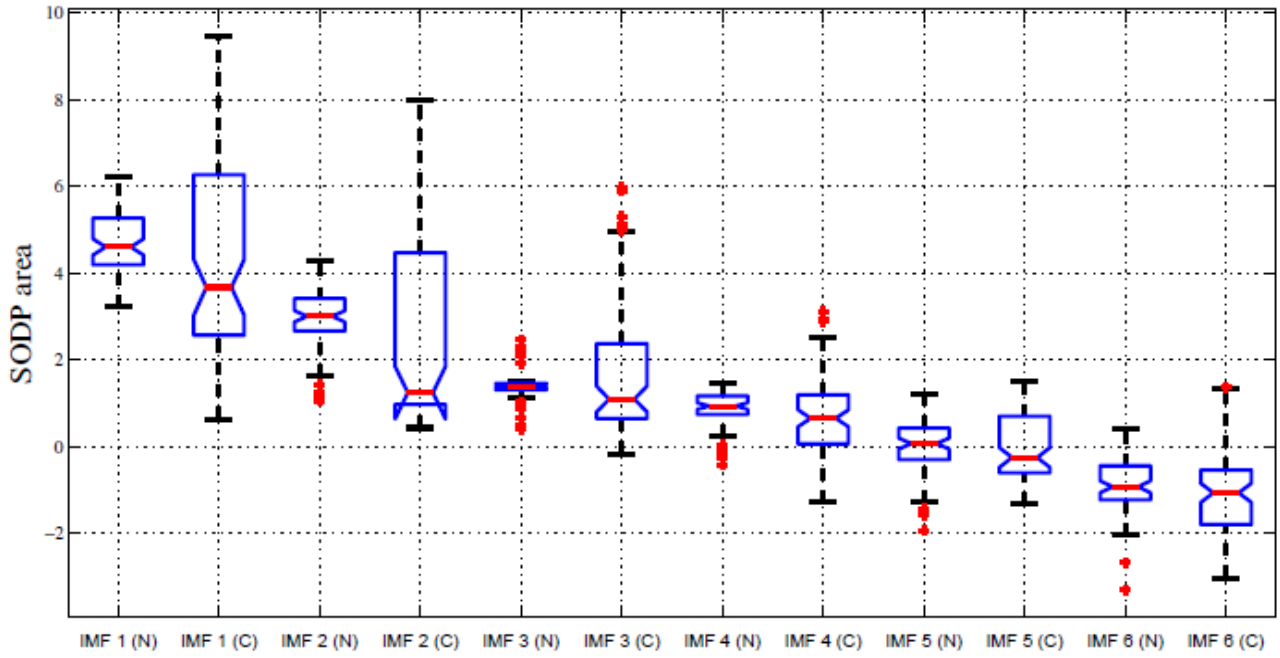

Figure 2.13: Box-plot of SODP area for normal and CAD heart rate signals with 250 samples.

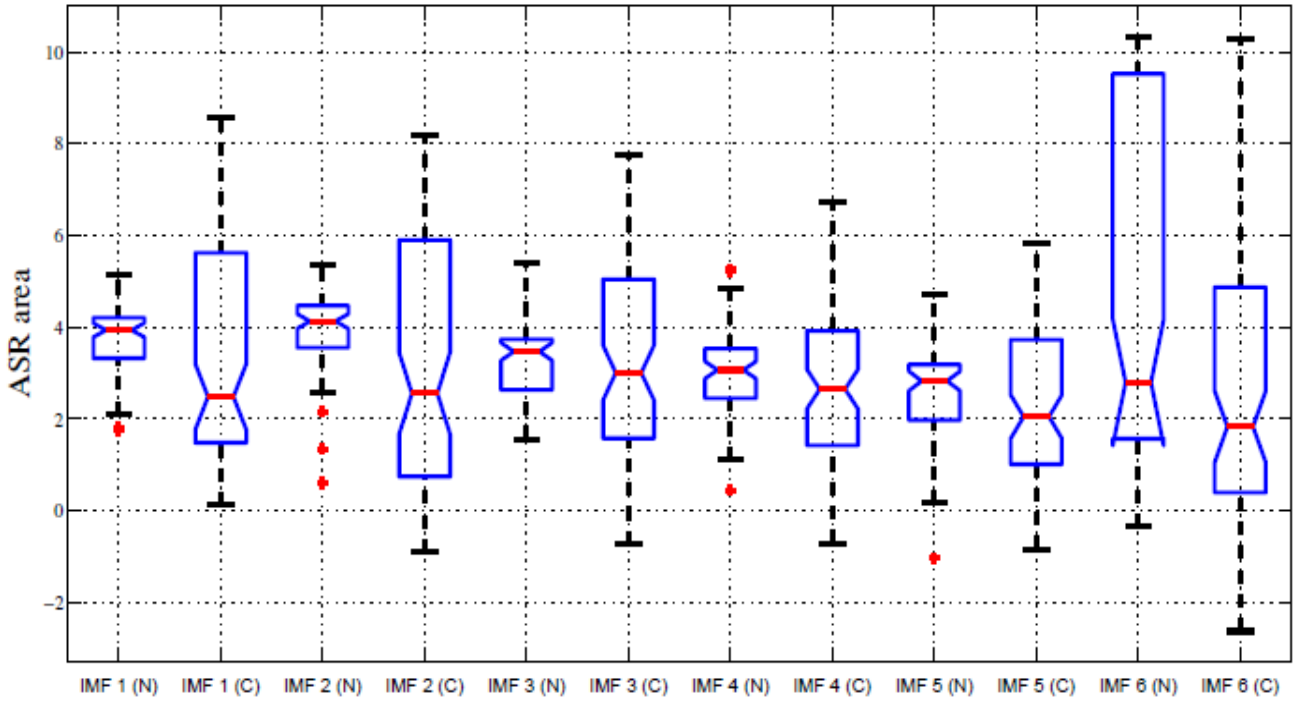

Figure 2.14: Box-plot of ASR area for normal and CAD heart rate signals with 250 samples.

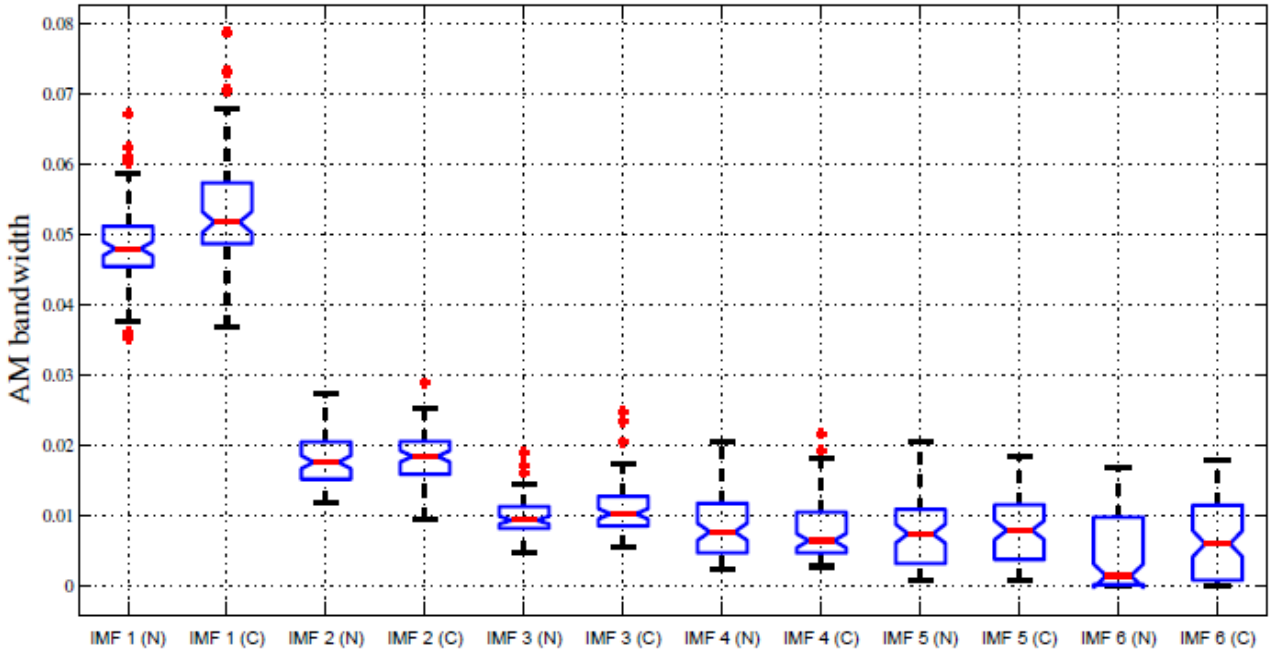

Figure 2.15: Box-plot of AM bandwidth for normal and CAD heart rate signals with 250 samples.

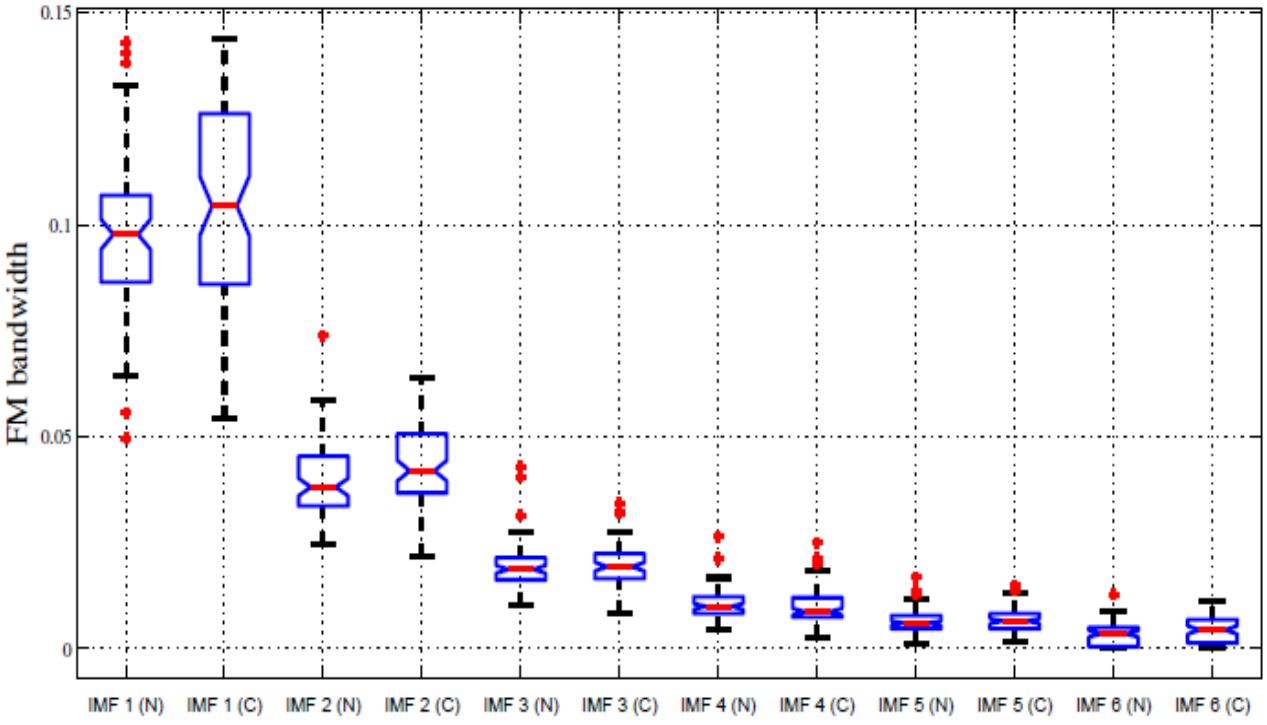

Figure 2.16: Box-plot of FM bandwidth for normal and CAD heart rate signals with 250 samples.

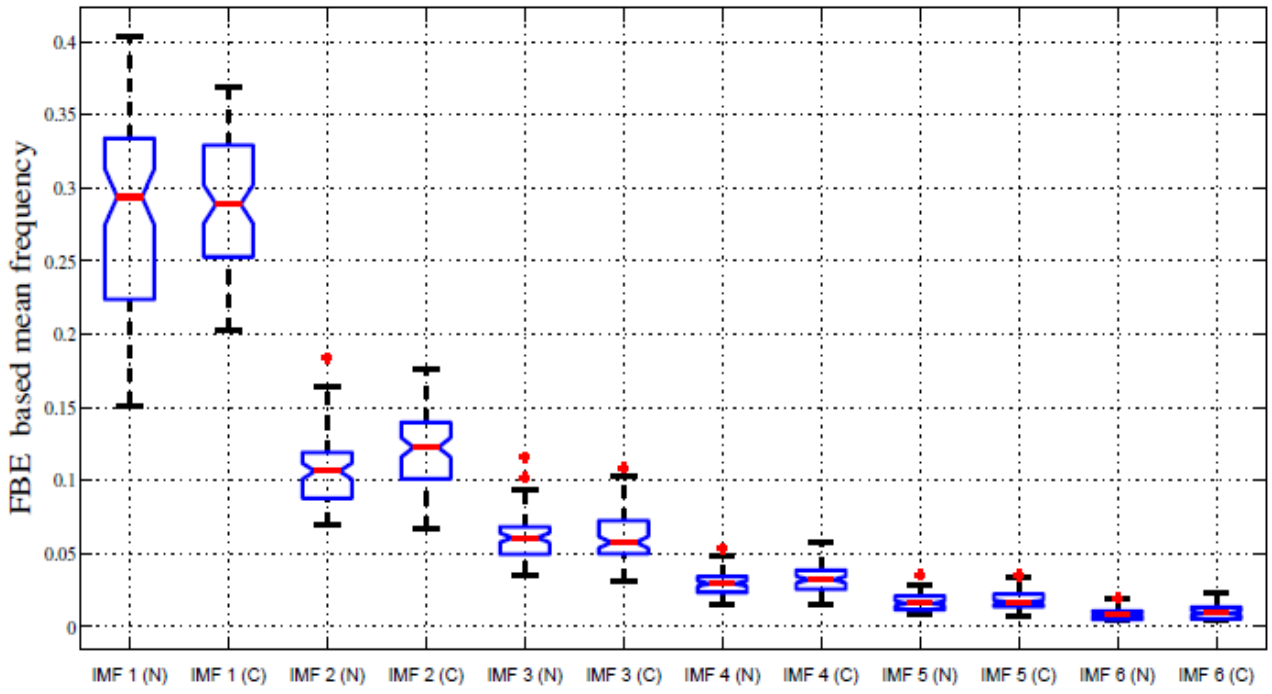

Figure 2.17: Box-plot of FBE based mean frequency for normal and CAD heart rate signals with 250 samples.

2.5 Discussion

The IMFs derived by EMD method from heart rate signals of normal and CAD subjects are arranged in a sequence of high frequency component to low frequency component. The five features obtained from these IMFs are tested using Kruskal-Wallis statistical test to analyze their statistical significance. The 95% ellipse area of SODP is used for analysis of normal and CAD signals. It can be observed from Table 2.1 that *p*-values for SODP area for all the IMFs are greater than 0.05 for signals with 1000 samples. Thus, for this case SODP area is not statistically significant for analysis of normal and CAD signals. For signal with 500 samples, it shows statistical significance ($p < 0.05$) for normal and CAD subjects for IMF 2 that can be observed in Table 2.2. It provides significant difference ($p < 0.05$) between normal and CAD heart rate signals for IMF 2, IMF 4 and IMF 6, in case of signal length of 250 samples which can be seen in Table 2.3.

For signal with 1000 samples, ASR area is not found to be statistically significant to distinguish normal and CAD heart rate signals. For each IMF, *p*-value for ASR area is greater than 0.05 which can be seen in Table 2.1. From Table 2.2, we can observe that for signal length of 500 samples normal and CAD heart rate signals are significantly discriminated ($p < 0.05$) based on ASR area for IMF 1, IMF 2 and IMF 6. Similarly, for signal length of 250 samples, the normal and CAD heart rate signals are differentiated significantly ($p < 0.05$) using ASR area parameter for first, second and sixth IMFs which is clear from Table 2.3.

The *p*-values of the AM bandwidth feature for IMF 1 and IMF 3 are significantly less ($p < 0.05$) for signals length of 1000 samples which can be observed from Table 2.1. Hence, IMF 1 and IMF 3 are suitable for discrimination of normal and CAD heart rate signals in this case. For signal length of 500 samples, *p*-values of AM bandwidth feature for IMF 1, IMF 3 and IMF 6 are significantly less ($p < 0.05$). Therefore, these IMFs are able to give significant difference for normal and CAD heart rate signals which can be seen in Table 2.2. It can be observed from Table 2.3 that, first IMF shows significantly less *p*-value ($p < 0.05$) corresponding to AM bandwidth feature. Hence differentiate significantly between normal and CAD heart rate signals in case of signal length of 250 samples.

The *p*-values of FM bandwidth feature for IMF 1, IMF 2 and IMF 4 to IMF 7 are significant ($p < 0.05$) for discrimination of normal and CAD heart rate signals, for signal length of 1000 samples which can be seen in Table 2.1. From Table 2.2, we can observe that for signal length of 500 samples the IMF 1, IMF 2 and IMF 4 have significantly less *p*-value ($p < 0.05$) for FM bandwidth parameter. Thus, provide significant difference for normal and CAD heart rate signals for this case. Similarly, IMF 2 and IMF 6 show significant difference ($p < 0.05$) for normal and CAD heart rate signals corresponding to FM bandwidth feature, in case of signal length of 250 samples which is clearly shown in Table 2.3.

From Table 2.1, we can observe significant difference for FBE-based mean frequency ($p < 0.05$) between normal and CAD heart arte signals for IMF 2 to IMF 7, in case of signal with 1000 samples. For signal length of 500 samples, normal and CAD heart rate signals are significantly differentiated using FBE-based mean frequency ($p < 0:05$) for IMF 2, IMF 4, IMF 5 and IMF 6 which is clear from Table 2.2. In case of signal length of 250 samples, IMF 2 and IMF 4 have lower *p*-values ($p < 0.05$) for FBE-based mean frequency. Therefore, able to significantly discriminate the normal and CAD heart rate signals which can be seen in Table 2.3.

CHAPTER 3

Empirical Wavelet Transform based Integrated Index for Normal and CAD Subjects

The objective of the work is to propose discrimination index for CAD and normal subjects using Empirical Wavelet Transform (EWT) [48] based features extracted from HRV signals. We have used the same data set as was used in the previous chapter. The same features are extracted after decomposing the heart rate signals using EWT. These features are SODP area, ASR area, AM bandwidth, FM bandwidth and FBE based mean frequency. The features are computed from the different modes extracted from HRV signals using EWT.

3.1 Motivation for using EWT

As shown in the previous chapter features namely: AM bandwidth, FM bandwidth and FBE based mean frequency are more suitable for the discrimination of normal and CAD signals. Recently, in order to have mathematical framework of the expansion process of the components, a new technique called empirical wavelet transform has been proposed in [48] which also extracts the amplitude modulated and frequency modulated (AM-FM) components of the signal using its Fourier spectrum. The Fourier spectrum is then segmented and filtering is applied to each segment thus generating different modes [48]. It should be noted that the EWT focuses mainly on the oscillatory behavior of the signal and thus the modes obtained from this decomposition are more consistent [48].

In the present work, we have used the EWT technique and obtained minimum of 3 modes for each signal as compared to the 7 IMFs obtained in the previous chapter. These 3 modes are much easier to interpret. The features namely: SODP area, ASR area, AM bandwidth, FM bandwidth and FBE based mean frequency were calculated from these obtained modes. These features were subjected to the Kruskal-Wallis statistical test to check their statistical significance. The *p*-values obtained using Kruskal-Wallis statistical test for the SODP area, ASR area, FM bandwidth and FBE based mean frequency features obtained from components using EWT method are shown in Table 3.1. The boxplots for the EWT are shown in Figure 3.1 to Figure 3.5.

Table 3.1: *p*-values of features extracted from different modes of normal and CAD signals using EWT.

Features	Mode 1	Mode 2	Mode 3
SODP area	2.8×10^{-4}	5.4×10^{-2}	3.9×10^{-1}
ASR area	1.7×10^{-3}	9.3×10^{-2}	5.8×10^{-1}
AM bandwidth	8.1×10^{-1}	2.5×10^{-1}	7.4×10^{-2}
FM bandwidth	5.9×10^{-3}	2.6×10^{-3}	8.5×10^{-1}
FBE based mean frequency	6.7×10^{-4}	1.2×10^{-1}	3.0×10^{-1}

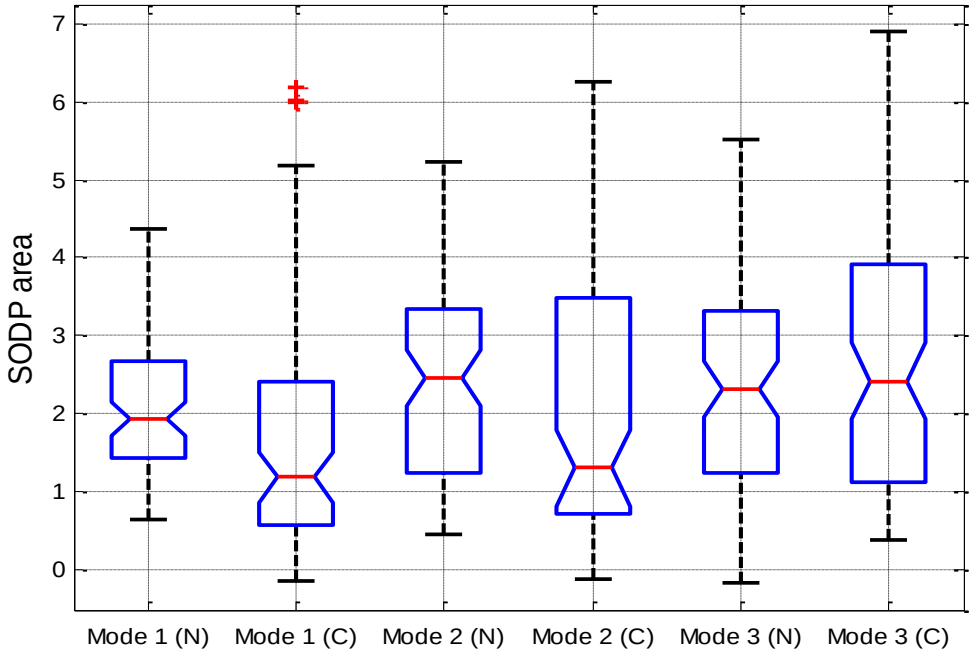

Figure 3.1: Boxplot of SODP area for normal and CAD signals using EWT.

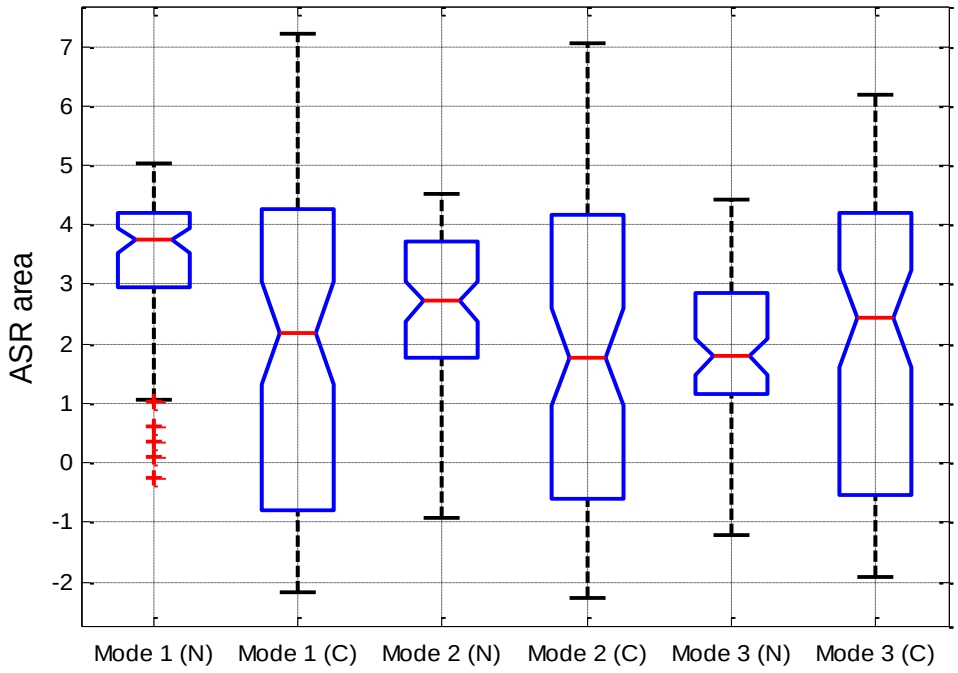

Figure 3.2: Boxplot of ASR area for normal and CAD signals using EWT.

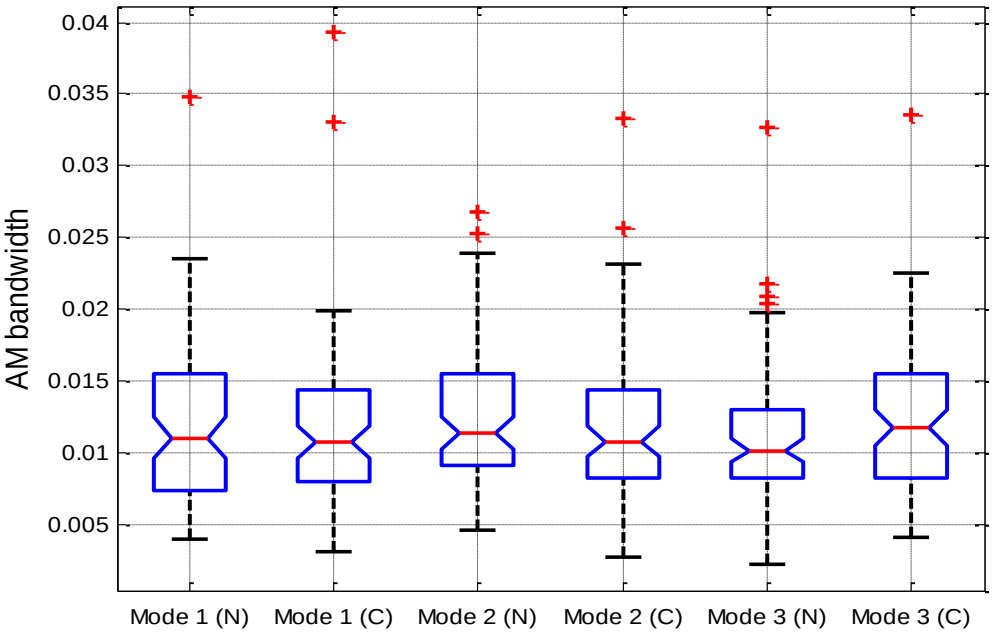

Figure 3.3: Boxplot of AM bandwidth for normal and CAD signals using EWT.

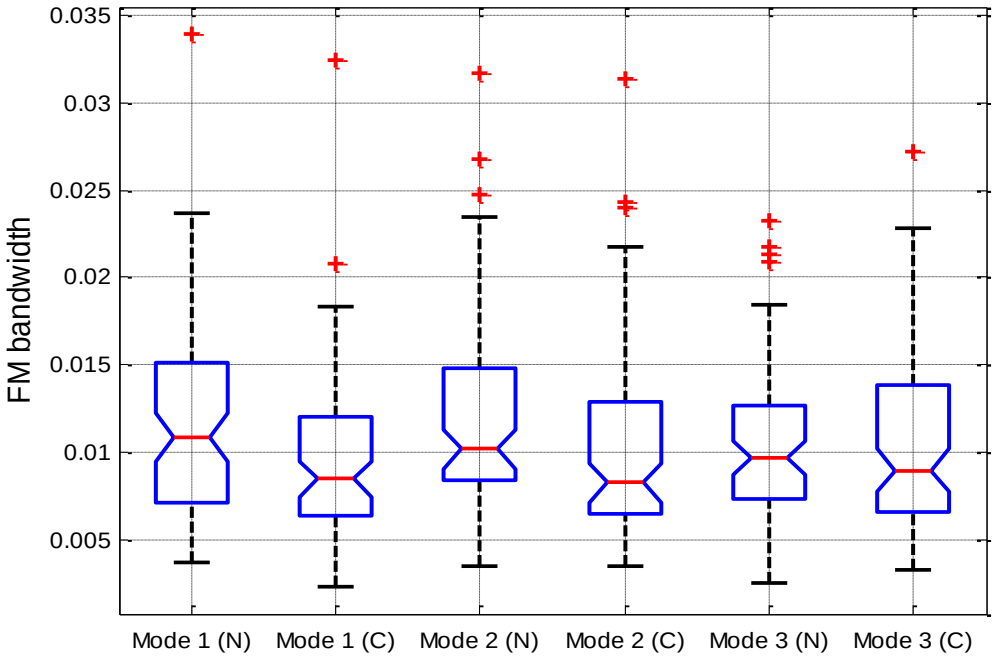

Figure 3.4: Boxplot of FM bandwidth for normal and CAD signals using EWT.

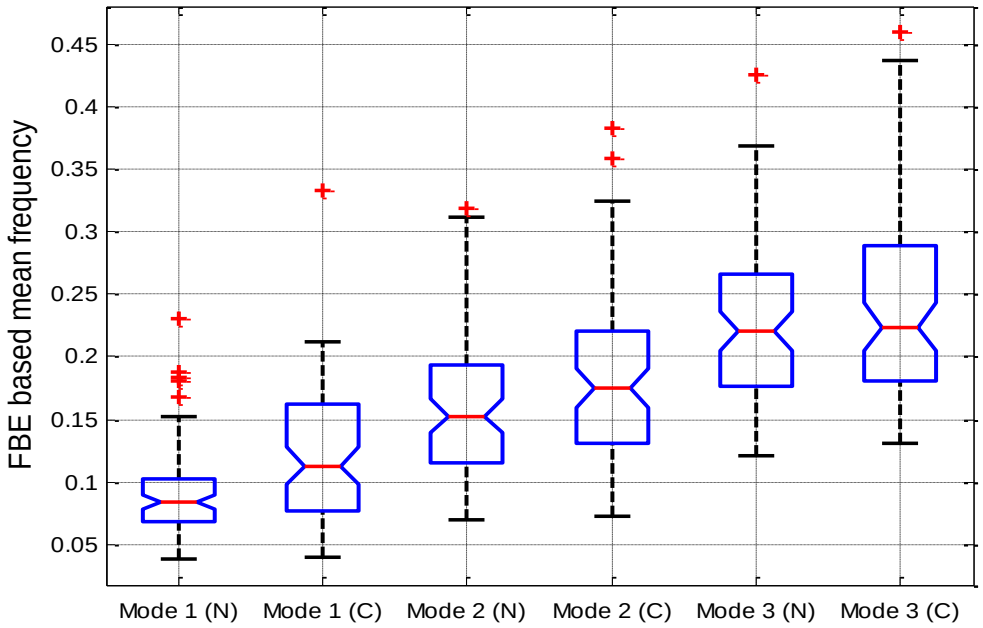

Figure 3.5: Boxplot of FBE based mean frequency for normal and CAD signals using EWT.

3.2 Empirical Wavelet Transform

The EWT [48] is a signal decomposition technique. It forms adaptive wavelets for extracting different modes of a signal. This method works as follows [48]: First, it uses fast Fourier transform (FFT) to determine the frequency components of the signal. Then, it segments the spectrum for extracting the different modes of the signal. Finally, it uses scaling and wavelet functions corresponding to each identified segment. EWT has also been successfully used in [23] for the diagnosis of glaucoma and extracting correntropy features from the affected patient's database.

The empirical scaling function $\phi_j(\omega)$ and the empirical wavelet $\psi_j(\omega)$ are given as follows [48]:

$$\phi_j(\omega_K) = \begin{cases} 1, & if\ |\omega_k| \leq\ (1-\lambda)\omega_j \\ \cos\left(\frac{\pi\alpha(\lambda,\omega_j)}{2}\right), & \text{if } (1-\lambda)\omega_j \leq |\omega_K| \leq (1+\lambda)\omega_j \\ 0, & \text{otherwise} \end{cases} \tag{3.1}$$

And,

$$\psi_j(\omega_K) = \begin{cases} 1, & \text{if } (1+\lambda)\omega_j \leq |\omega_K| \leq (1-\lambda)\omega_j \\ \cos\left(\frac{\pi\alpha(\lambda,\omega_{j+1})}{2}\right), & \text{if } (1-\lambda)\omega_{j+1} \leq |\omega_K| \leq (1+\lambda)\omega_{j+1} \\ \sin\left(\frac{\pi\alpha(\lambda,\omega_j)}{2}\right), & \text{if } (1-\lambda)\omega_j \leq |\omega_K| \leq (1+\lambda)\omega_j \\ 0, & \text{otherwise} \end{cases} \tag{3.2}$$

Where,

$$\alpha(\lambda,\omega_j) = \alpha\left(\frac{|\omega_K|-(1-\lambda)\omega_j}{2\lambda\omega_j}\right) \tag{3.3}$$

To obtain tight frame of wavelets, the λ parameter must satisfy the following condition [48]:

$$\lambda < \ min_m \left(\frac{\omega_{j+1} - \omega_j}{\omega_{j+1} + \omega_j} \right) \tag{3.4}$$

And $\alpha(x)$ is an arbitrary function defined as [48]:

$$\alpha(x) = \begin{cases} 0, & \text{if } x \leq 0 \\ \alpha(x) + \alpha(1-x) = 1, & \forall\, x \in [0,1] \\ 1, & \text{if } x \geq 1 \end{cases} \tag{3.5}$$

3.3 Formulation of Integrated Index

To distinguish HRV signals of CAD and normal classes, an expression can be derived using significant features. This expression provides a unique range of values for each class [49, 50]. Therefore, discrimination between two classes can be performed using only a single index. In present work, we used significant features to derive the integrated discrimination index, namely the CAD and normal index (CAD-N). The expression for CAD-N is derived on the basis of trial and error experimentation and given as:

$$\text{CAD-N} = \text{A x m1- C x m3+ B x m2} \tag{3.6}$$

Where, m1, m2 and m3 are the values of the three most significant features extracted from CAD and normal HRV signals. In the above expression, A, B and C are the variables and optimized to achieve a unique range of CAD-N index for both the classes. In present work, genetic algorithm [16] is used to find the optimum value of the variables A, B and C.

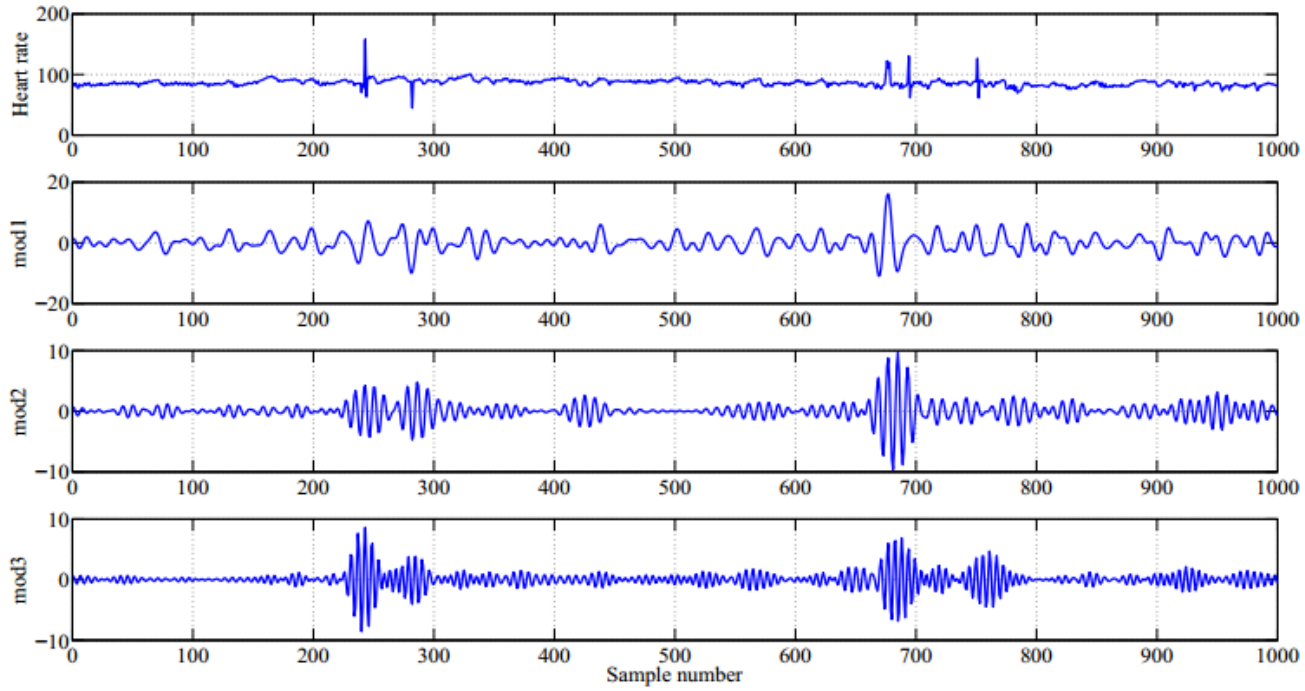

(a)

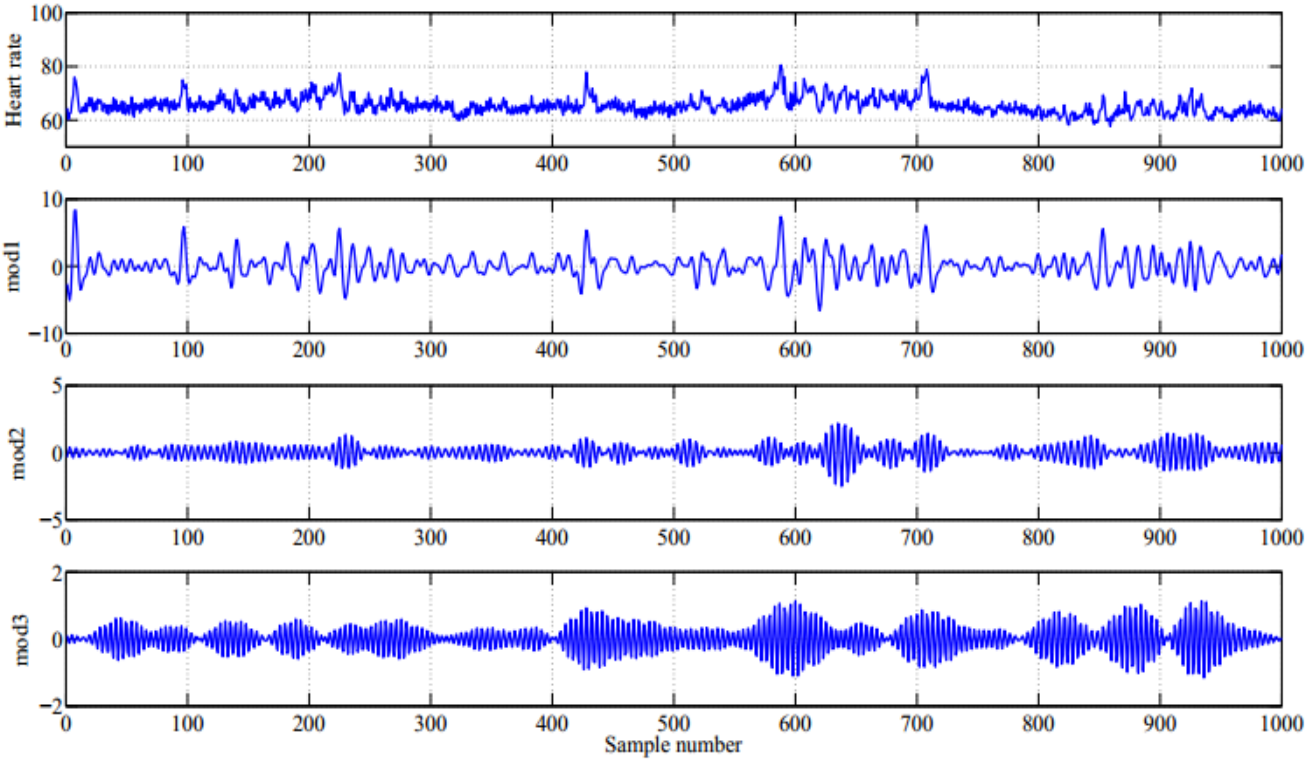

(b)

Figure 3.6: First 3 modes of heart rate signal of (a) CAD subject and (b) Normal subject.

3.4 Results and Discussion

In the present work, CAD and normal HRV signals are decomposed using EWT and each mode is used to extract the features. We used scalespace parameter detection method [48] to decompose HRV signals into the maximum modes and we have used the available matlab codes for EWT from [51]. Three modes were observed in each HRV signal of both classes. Hence, three modes are taken to analyze these signals. These modes can be seen in Figure 3.6. Further, five features namely; SODP area, ASR area, AM bandwidth, FM bandwidth, and FBE based *mean* frequency are computed from these modes. The mean and standard deviation (SD) of all features for the three extracted modes are calculated. In our work, we used Student's t-test ranking method [14] to select the most significant features. In this method, population mean is computed and used to find the discrimination between two classes. On performing this test, t-values are obtained. The feature which has higher t value that has the most ability to discriminate the two classes [14]. Further, CAD-N index are derived using first three most significant features, and this index is shown in Figure 3.7

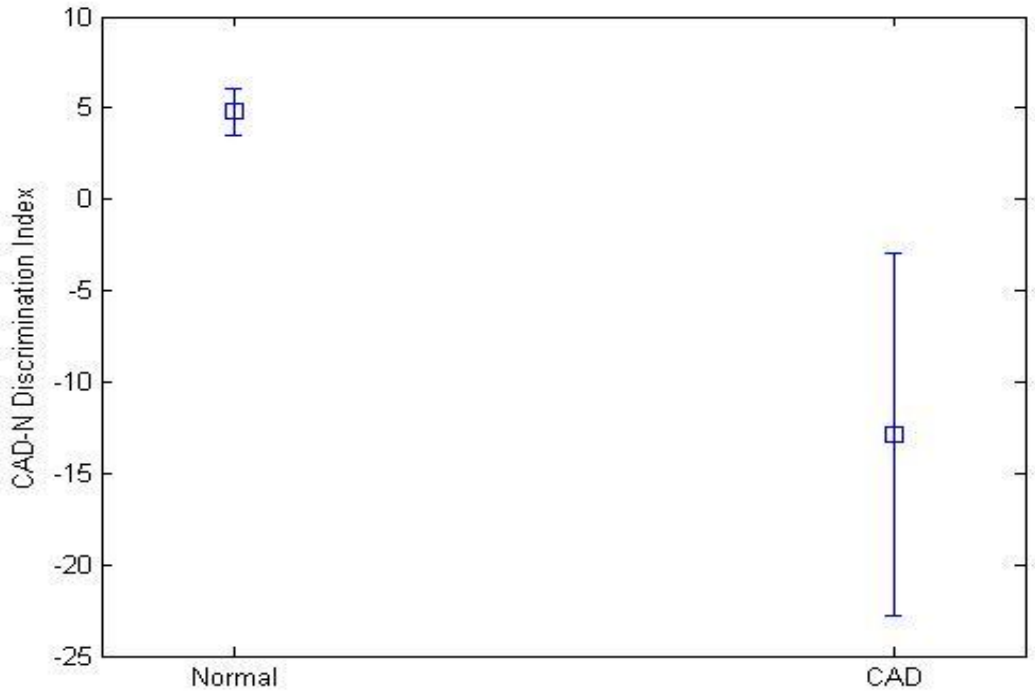

Figure 3.7: The ranges of CAD-N index for heart rate signals of normal and CAD subjects.

CHAPTER 4

Conclusion and Future Scope

4.1 Conclusion

In this work we have proposed features for automated discrimination of normal and CAD subjects using heart rate signals. We have used EMD method to decompose the heart rate signals into IMFs, and features namely SODP area, ASR area, AM bandwidth, FM bandwidth and FBE-based mean frequency are extracted from these IMFs. These features are studied for different sample lengths of 1000, 500 and 250 respectively. Effectiveness of these features are also evaluated using Kruskal-Wallis statistical test. The feature which has *p*-value less than 0.05 is considered to be statistically significant, and can be used to discriminate between the two classes. For signal length of 1000, 500 and 250 samples, AM bandwidth feature has least *p*-value for first IMF. Results show that the features namely; AM bandwidth, FM bandwidth, and FBE-based mean frequency for signal with 1000 samples are found to be more suitable to discriminate normal and CAD heart rate signals compared to ASR area and SODP area features.

We have also proposed CAD-N index for automated discrimination of normal and CAD subjects based on HRV signals. EWT method is used to decompose the HRV signals. Features namely SODP area, ASR area, AM bandwidth, FM bandwidth, and FBE based mean frequency are computed from the first three modes extracted using EWT. Features are ranked using Student t-test ranking method. First three ranked features are used to derive the CAD-N index, which is able to clearly separate the two classes.

4.2 Future Scope

We have used small dataset in the present work. In future this proposed methodology could be used to study large dataset before applying it to the clinical purpose. The real time implementation of this work can save the time of doctors and can be made cost effective. Moreover, this methodology can be used for the diagnosis of other diseases such as myocardial infractions, atrial fibrillation and many more.

References

[1]. Wong ND, "Epidemiological studies of CHD and the evolution of preventive cardiology," *Nat. Rev. Cardiol.,* vol. 11, pp. 276–289, 2014.

[2]. National Heart, Lung and Blood Institute, What is coronary heart disease? 2011, Available at http://www.nhlbi.nih.gov/health/health-topics/topics/cad/ (accessed 2016-06-16 June 2016).

[3] World Health Organization: Cardiovascular diseases, 2015. URL: http: //www.who.int/mediacentre/factsheets/fs317/en/, accessed 2016-03-01.

[4] Biel L., Pettersson O., Philipson L., and Wide P., "ECG analysis: a new approach in human identification," *IEEE Transactions on Instrumentation and Measurement,* vol. 50, no. 3, pp. 808– 812, 2001.

[5]. Giri D, Acharya U. R, Martis R. J, Sree S. V, Lim T. C, Suri J. S, "Automated diagnosis of coronary artery disease affected patients using LDA, PCA, ICA and discrete wavelet transform," *Knowledge Based System,* vol. 37, pp. 274–282, 2013.

[6]. Acharya U. R, Faust O, Sree V, Swapna G, Martis R. J, Kadri N. A, Suri J. S, "Linear and nonlinear analysis of normal and CAD-affected heart rate signals," *Computer Methods Prog. Biomed.*, vol. 113, pp. 55–68, 2014.

[7]. Acharya U. R, Kannathal N, Krishnan S. M, "Comprehensive analysis of cardiac health using heart rate signals," *Physiol. Meas.,* vol. 25, pp. 1139–1151, 2004.

[8]. Huikuri H. V, Niemela M. J, Ojala S, Rantala A, Ikaheimo M. J, Airaksinen K. E, "Circadian rhythms of frequency domain measures of heart rate variability in healthy subjects and patients with coronary artery disease. Effects of arousal and upright posture," *Circulation,* vol. 90, pp. 121–126, 1994.

[9]. Bigger J. T, Fleiss J. L, Steinman R. C, Rolnitzky L. M, Schneider W. J, Stein P. K, "RR variability in healthy, middle-aged persons compared with patients with chronic coronary heart disease or recent acute myocardial infarction," *Circulation,* vol. 91, pp. 1936–1943, 1995.

[10]. Acharya U. R, Bhat P. S, Kannathal N, Rao A, Lim C. M, "Analysis of cardiac health using fractal dimension and wavelet transformation," *ITBM-RBM,* vol. 26, pp. 133–139, 2005.

[11]. Karamanos K, Nikolopoulos S, Hizanidis K, Manis G, Alexandridi A, Nikolakeas S, "Block entropy analysis of heart rate variability signals," *Int. J. Bifurcat. Chaos,* vol. 16, pp. 2093– 2101, 2006.

[12]. Antanavicius K., Bastys A., Bluzas J., Gargasas L., Kaminskiene S, Urbonaviciene G., Vainoras A., "Nonlinear dynamics analysis of electrocardiograms for detection of coronary artery disease," *Computer Methods and Programs in Biomedicine,* vol. 92, pp. 198–204, 2005.

[13] Patidar S, Pachori R. B, Acharya U. R, "Automated diagnosis of coronary artery disease using tunable-Q wavelet transform applied on heart rate signals," *Knowl. Based Syst.*, vol. 82, pp. 1– 10, 2015.

[14]. Zhu W., Wang X., Ma Y., Rao M., Glimm J., Kovach J. S., "Detection of cancer-specific markers amid massive mass spectral data" vol. 100, pp. 14666–14671, 2003.

[15]. Chua K. C, Chandran V, Acharya U. R, Lim C. M, "Cardiac state diagnosis using higher order spectra of heart rate variability," *J Med Eng Technol,* vol. 32, pp. 145–155, 2008.

[16]. Babaoglu I, Findik O, Ulker E, "A comparison of feature selection models utilizing binary particle swarm optimization and genetic algorithm in determining coronary artery disease using support vector machine," *Expert Syst. Appl.*, vol. 37, pp. 3177–3183, 2010.

[17]. Lee H. G, Noh K. Y, Ryu K. H, "Mining bio-signal data: Coronary artery disease diagnosis using linear and nonlinear features of HRV," *Emerging Technologies in Knowledge Discovery and Data Mining, Lecture Notes in Computer Science*, vol. 4819, pp. 218–228, 2007.

[18]. McKight P. E, Najab J, "Kruskal-Wallis test," *Corsini Encyclopedia of Psychology*, John Wiley & Sons, 2010.

[19]. BIOPAC Systems Canada, Inc., Acknowledge 4.1, BIOPAC Systems, Inc., 2010, Available at http://www.biopac.ca/Acqknowledge 40.htm.

[20]. Warlar R, Eswaran C, "Integer coefficient bandpass filter for the simultaneous removal of baseline wander, 50 and 100 Hz interference from the ECG," *Med. Biol. Eng. Computer,* vol. 29, pp. 333–336, 1991.

[21]. Pan J, Tompkins W. J, A real-time QRS detection algorithm, *IEEE Trans. Biomed. Eng.*, vol. 32, pp. 230–236, 1985.

[22]. Huang N. E, Shen Z, Long S. R, Wu M. C, Shih H. H, Zheng Q, Yen N. C, Tung C. C, Liu H. H, "The empirical mode decomposition and the Hilbert spectrum for nonlinear and non-stationary time series analysis," *Proc. R. Soc. Lond. A Math. Phys. Eng. Sci.*, vol. 454, pp. 903–995, 1998.

[23]. Maheshwari S., Pachori R.B., and Acharya U.R., "Automated diagnosis of glaucoma using empirical wavelet transform and correntropy features extracted from fundus images," *IEEE Journal of Biomedical and Health Informatics*, in press, 2016.

[24]. Thuraisingham R. A, Tran Y, Boord P, Craig A, "Analysis of eye open, eye closed EEG signals using second order difference plot," *Med. Biol. Eng. and Computer*, vol. 45, pp 1243–1249, 2007.

[25]. Cohen M. E, Hudson D. L, Deedwania P. C, "Applying continuous chaotic modeling to cardiac signal analysis," *Eng. Med. Bio. Mag.*, vol. 15, pp. 97–102, 1996.

[26]. Prieto T. E, Myklebust J. B, Hoffmann R. G, Lovett E. G, Myklebust B. M, "Measures of postural steadiness: Differences between healthy young and elderly adults," *IEEE Trans. Biomed. Eng.* vol. 43, pp. 956–966, 1996.

[27]. Cavalheiro G. L, Almeida M. F. S, Pereira A. A, Andrade A. O, "Study of age-related changes in postural control during quiet standing through linear discriminant analysis," *Biomed. Eng. Online*, vol. 8, pp. 1–3, 2009.

[28]. Pachori R. B, Hewson D, Snoussi H, Ducene J, "Postural time-series analysis using empirical mode decomposition and second-order difference plots," *IEEE Int. Conf. Acoustics, Speech and Signal Processing*, Taipei, Taiwan, pp. 537–540, 2009.

[29]. Pachori R. B, Patidar S, "Epileptic seizure classification in EEG signals using second-order difference plot of intrinsic mode functions," *Comput. Methods Prog. Biomed.*, vol. 113, pp. 494– 502, 2014.

[30]. Pachori R. B, Sharma R, Patidar S, "Classification of normal and epileptic seizure EEG signals based on empirical mode decomposition," *Complex System Modelling and Control Through Intelligent Soft Computations, Studies in Fuzziness and Soft Computing*, vol. 319, pp. 367–388, 2015.

[31]. Pachori R. B, Avinash P, Shashank K, Sharma R, Acharya U. R, "Application of empirical mode decomposition for analysis of normal and diabetic RR-interval signals," *Expert Syst. Appl.* vol. 42, pp. 4567–4581, 2015.

[32]. Y.-C. Lai, N. Ye, "Recent developments in chaotic time series analysis*," Int. J. Bifurcat. and Chaos,* vol. 13, pp. 1383–1422, 2003.

[33]. Pachori R. B, Bajaj V, "Analysis of normal and epileptic seizure EEG signals using empirical mode decomposition," *Comput. Methods Prog. Biomed.* vol. 104, pp. 373–381, 2011.

[34]. Amoud H, Snoussi H, Hewson D. J, J. Duchene, "Hilbert-Huang transformation: Application to postural stability analysis," *IEEE Int. Conf. Engineering in Medicine and Biology*, Lyon, pp. 1562–1565, 2007.

[35]. Parey A, Pachori R. B, "Gear fault diagnosis based on central tendency measure of intrinsic mode functions," *Int. J. COMADEM,* vol. 17, pp. 15–22, 2014.

[36]. Amoud H, Snoussi H, Hewson D. J, Duchene J, "Univariate and bivariate empirical mode decomposition for postural stability analysis," *EURASIP J. Adv. Signal Processing,* pp. 1–11, 2008.

[37]. Cohen L, Lee C, "Instantaneous bandwidth for signals and spectrogram," *Int. Conf. Acoustics Speech and Signal Processing,* pp. 2451–2454, 1990.

[38]. Bajaj V, Pachori R. B, "Classification of seizure and nonseizure EEG signals using empirical mode decomposition," *IEEE Trans. Inf. Technol. Biomed.,* vol. 16, pp. 1135–1142, 2012.

[39]. Pachori R. B, "Discrimination between ictal and seizure-free EEG signals using empirical mode decomposition," *Res. Lett. Signal Process,* pp. 1-5, 2008.

[40]. Pachori R. B, Hewson D. J, Snoussi H, Duchene J, "Analysis of center of pressure signals using empirical mode decomposition and Fourier-Bessel expansion," *IEEE Region 10 TENCON Conf.,* Hyderabad, pp. 1–6, 2008.

[41]. Schroeder J, "Signal processing via Fourier-Bessel series expansion," *Digital Signal Process,* vol. 3, pp. 112–124, 1993.

[42]. Pachori R. B, Sircar P, "A new technique to reduce cross terms in the Wigner distribution," *Digital Signal Process,* vol. 17, pp. 466–474, 2007.

[43]. Pachori R. B, Sircar P, "EEG signal analysis using FB expansion and second-order linear TVAR process," *Signal Process*, vol. 88, pp. 415–420, 2008.

[44]. Pachori R. B, Sircar P, "Analysis of multicomponent AM-FM signals using FB-DESA method," *Digital Signal Process*, vol. 20, pp. 42–62, 2010.

[45]. Jain P, Pachori R. B, "Event-based method for instantaneous fundamental frequency estimation from voiced speech based on eigenvalue decomposition of the Hankel matrix," *IEEE/ACM Trans. Audio Speech Lang. Process.* vol. 22, pp. 1467–1482, 2014.

[46]. Gopalan K, Anderson T. R, Cupples E. J, "A comparison of speaker identification results using features based on cepstrum and Fourier-Bessel expansion," *IEEE Trans. Speech Audio Process*, vol. 7, pp. 289–294, 1999.

[47]. Hood A. S, Pachori R. B, Reddy V. K, Sircar P, "Parametric representation of speech employing multi-component AFM signal model*," Int. J. Speech Technol.* Vol. 18, pp. 287–303, 2015.

[48] Gilles J., "Empirical wavelet transform," *IEEE Transactions on Signal Processing*, vol. 61, pp. 3999–4010, 2013.

[49] Ghista D. N., "Physiological systems; numbers in medical diagnosis and hospital cost-effective operation," *Journal of Mechanics in Medicine and Biology*, vol. 4, pp. 401–418, 2005.

[50] Acharya U. R., Faust O., Sree S. V., Ghista D. N., Dua S., Joseph P., Ahamed V. I. T., Janarthanan N, Tamura T., "An integrated diabetic index using heart rate variability signal features for diagnosis of diabetes," *Computer Methods in Biomechanics and Biomedical Engineering*, vol. 16, pp. 222–234, 2013.

[51]. MathWorks, Empirical wavelet transform, Gilles J., URL: https://www.in.mathworks.com/matlabcentral/fileexchange/42141-empirical-wavelet-transforms